LATERAL BRANCHING OXIDOREDUCTASE specificity for strigolactone branching inhibition in barley

Maiko Inoue[1], Apriadi Situmorang[2], Jack H. Kelly[2], Weiwei Chen[2], Hui Zhou[2], Carlotta C. Ferrario[3,4], Veronica Gregis[3], Alessandro Vajani[4], Salar Shaaf[4,5], Abhisek Biswas[4], Rana Alqusumi[6], Mark T. Waters[6], Matthew R. Tucker[2,7,8], Dabing Zhang[2,7], Stephanie J. Watts-Williams[2,8], Agnieszka Janiak[9], Marek Marzec[9], Beata Chmielewska[9], Laura Rossini[4], Kaori Yoneyama[1], Philip B. Brewer[2,8,10,11]

[1] Department of Biochemistry and Molecular Biology, Saitama University, 255 Shimo-Okubo, Sakura-ku, Saitama 338-8570, Japan

[2] Waite Research Institute, School of Agriculture Food & Wine, The University of Adelaide, Adelaide, SA 5064, Australia

[3] University of Milan, Department of Biosciences, Via Celoria 26, 20133 Milan, Italy

[4] University of Milan, Department of Agricultural and Environmental Sciences (DiSAA), Via Celoria 2, 20133 Milan, Italy

[5] Leibniz Institute of Plant Genetics and Crop Plant Research (IPK) Gatersleben, 06466 Seeland, Germany

[6] School of Molecular Sciences, The University of Western Australia, Perth WA 6009, Australia

[7] ARC Training Centre for Future Crops Development, The University of Adelaide, Adelaide, SA 5064, Australia

© The Author(s) 2025. Published by Oxford University Press on behalf of Society for Experimental Biology. This is an Open Access article distributed under the terms of the Creative Commons Attribution-NonCommercial License (https://creativecommons.org/licenses/by-nc/4.0/), which permits non-commercial re-use, distribution, and reproduction in any medium, provided the original work is properly cited. For commercial re-use, please contact reprints@oup.com for reprints and translation rights for reprints. All other permissions can be obtained through our RightsLink service via the Permissions link on the article page on our site—for further information please contact journals.permissions@oup.com.

ACCEPTED MANUSCRIPT

Downloaded from https://academic.oup.com/jxb/advance-article/doi/10.1093/jxb/eraf285/8174788 by guest on 10 July 2025

[8] Australian Research Council Centre of Excellence in Plants for Space, The University of Adelaide, Adelaide, SA 5064, Australia

[9] University of Silesia in Katowice, Institute of Biology, Biotechnology and Environmental Protection, Jagiellonska 28, 40032 Katowice, Poland

[10] Institute for Future Farming Systems, Central Queensland University, Rockhampton, QLD 4701, Australia

[11] La Trobe Institute for Sustainable Agriculture and Food, La Trobe University, Bundoora, VIC 3086, Australia

*Corresponding author: Philip B. Brewer, email: philip.brewer@adelaide.edu.au

Highlight

Barley *lateral branching oxidoreductase* mutants reveal functional divergence between strigolactones involved in tillering and those involved in root exudates.

Abstract

Strigolactone (SL) mutants display a range phenotypes, such as increased branching, reduced stature and a loss of SLs exuded from roots into soil. SL biosynthesis is complex and divergent between plant species. Recently, mutants defective in specific SL biosynthesis genes have shown a loss of exuded SLs, but no obvious change in branching (tillering). This means that functional specification may exist between certain SL sub-types. It has been suggested that the LATERAL BRANCHING OXIDOREDUCTASE (LBO) enzyme acts in a sub-pathway of SLs that is specific for

ACCEPTED MANUSCRIPT

Downloaded from https://academic.oup.com/jxb/advance-article/doi/10.1093/jxb/eraf285/8174788 by guest on 10 July 2025

branching. Here we report that barley plants mutants in *hvlbo* have increased tillering, but normal production of SLs detected in roots and root exudates. This finding supports the idea that SLs have functional or tissue-specific differences and that the LBO pathway has specificity for bud outgrowth rather than exudates.

Key words

Strigolactone, biosynthesis, branching, tillering, root exudate, barley, crop, yield

Abbreviations

SL, strigolactone; D14, DWARF14; CLAMT, CLA METHYLTRANSFERASE; LBO, LATERAL BRANCHING OXIDOREDUCTASE; TILLING, Targeting Induced Local Lesions in Genomes; WT, wild type; *Hor*TILLUS, *Hordeum vulgare* TILLING University of Silesia; CDS, coding sequence; CaMV, Cauliflower Mosaic Virus; SD, short-day; LD, long-day; AM, arbuscular mycorrhizal; 2-OGD, 2-oxoglutarate and Fe(II)-dependent dioxygenase; DSBH, double-stranded β-helix conserved catalytic domain; GP, Golden promise; Seb, Sebastian, CL, carlactone; CLA, carlactonoic acid; MeCLA, methyl carlactonoate; 1'-HO-MeCLA, hydroxymethyl carlactonoate.

Introduction

Strigolactone (SL) biosynthesis consists of a core conserved pathway from β-carotene to carlactone (CL), which then diverges through a range of enzymatic pathways to produce various SL types depending on each plant species (Dun *et al.*, 2023; Marzec *et*

ACCEPTED MANUSCRIPT

Downloaded from https://academic.oup.com/jxb/advance-article/doi/10.1093/jxb/eraf285/8174788 by guest on 10 July 2025

al., 2020b; Nomura *et al.*, 2024; Yoneyama and Brewer, 2021). SLs are plant hormones perceived by the DWARF14 (D14) receptor, which is encoded by a single gene copy in most species (Waters *et al.*, 2012). Mutants that fail to produce the core biosynthesis pathway, such as rice *dwarf17* (*d17*) or maize *zmccd8*, display the full range of SL-related phenotypes, such as excessive branching/tillering, dwarfism and the absence of SLs exuded from roots (Brewer *et al.*, 2013; Chen *et al.*, 2023; Ito *et al.*, 2022; Li *et al.*, 2023). Failure to exude SLs can result in reduced fungal symbiosis or parasitic weed infestation (Gomez-Roldan *et al.*, 2008; Umehara *et al.*, 2008). SLs, including those that are exuded, can inhibit branching when artificially added onto buds (Arite *et al.*, 2009). Hence, it has been assumed that any SL exuded from roots, also contributes to branching inhibition as an internal hormone. However, recently, SL mutants have been reported to be defective in exudates (and some plant phenotypes), but normal in branching/tillering (Chen *et al.*, 2023; Ito *et al.*, 2022; Li *et al.*, 2023; Li *et al.*, 2024; Wakabayashi *et al.*, 2019; Wang *et al.*, 2024; Zhou *et al.*, 2025).

The phenotypic separation of exudate content and shoot branching suggests there are SL biosynthesis pathways for distinctive compounds with different physiological functions. For instance, Os900 is a CYP711A2 enzyme in rice involved in the production of deoxyorobanchol (4DO), which is further converted to orobanchol (oro) by Os1400 (CYP711A3). However, although rice *os1400* and/or *os900* mutants showed loss of SL exudate, they did not show the increased tillering phenotype of the core biosynthesis mutant, *d17* (Chen *et al.*, 2023; Ito *et al.*, 2022). Moreover, *os1400* single mutants were specifically shorter due to a build-up of 4DO (Chen et al., 2023). In maize,

ACCEPTED MANUSCRIPT

Downloaded from https://academic.oup.com/jxb/advance-article/doi/10.1093/jxb/eraf285/8174788 by guest on 10 July 2025

ZmCYP706C37 and ZmMAX1b (a CYP711A enzyme) are required for the production of prominent exuded SLs, including zealactone. However, plants defective in those enzymes did not show the branching increase that was observed in the core biosynthesis mutant, *zmccd8* (Li *et al.*, 2023). Also, OsCYP706C2 and two methyl transferases are involved in converting CL to 4-oxo-methyl carlactonoate (4-oxo-MeCLA). However, although *oscyp706c2* mutants were defective in 4-oxo-MeCLA exudate, root mycorrhizal colonization and root architecture, they did not show increased tillering (Li *et al.*, 2024). CYP722C is involved in the production of oro. In tomato, loss of *slcyp722c* caused deficiencies of oro and solanacol in exudates, but did not affect branching or height (Wakabayashi *et al.*, 2019). Moreover, recent findings showed that CYP722A converts carlactonoic acid (CLA) into 16-hydroxy-CLA. However, Arabidopsis *atcyp722a* mutants showed no increase in branching (Zhou *et al.*, 2025).

The production and identity of hormone-specific SLs remains unclear, together with how they may function specifically in branching. The most-likely pathway involves the enzymes CLA METHYLTRANSFERASE (CLAMT) and LATERAL BRANCHING OXIDOREDUCTASE (LBO) (Brewer *et al.*, 2016; Haider *et al.*, 2023; Li *et al.*, 2023; Mashiguchi *et al.*, 2022; Wakabayashi *et al.*, 2021; Yoneyama *et al.*, 2020a; Zhou *et al.*, 2025). CLAMT is a methyl-transferase that catalyzes CLA to MeCLA. Arabidopsis *atclamt* mutants still produced CLA, but were deficient in MeCLA, and yet showed increased branching (Mashiguchi *et al.*, 2022; Wakabayashi *et al.*, 2021).

ACCEPTED MANUSCRIPT

Downloaded from https://academic.oup.com/jxb/advance-article/doi/10.1093/jxb/eraf285/8174788 by guest on 10 July 2025

MeCLA can be further converted to 1'-OH-MeCLA by LBO, which is a 2-oxoglutarate and Fe(II)-dependent dioxygenase (2-OGD) (Brewer *et al.*, 2016; Yoneyama *et al.*, 2020a; Zhou *et al.*, 2025). However, the role of 1'-OH-MeCLA is uncertain (Brewer et al., 2016). Arabidopsis *atlbo* mutants still produced upstream compounds CL and MeCLA, and yet branching was not fully repressed (Brewer et al., 2016). This means that LBO produces from MeCLA one or more SLs that inhibit branching, which contrasts with the pathway steps described above that relate to SL exudates, but not branching. Moreover, *clamt* and *lbo* double mutant plants were additive in branching, attaining the same level as the core biosynthesis mutant, *atccd7* (Zhou et al., 2025). This confirms that the CLAMT-LBO pathway is a key regulator of branching, and MeCLA bioactivity is enhanced by LBO for full branching inhibition.

Hydroxylated versions of CLA can also be processed into hydroxylated derivatives by CLAMT and LBO (Yoneyama et al. 2020a; Zhou et al., 2025). Accordingly, a group of related compounds could be produced internally in plants as branching inhibitors (Zhou et al., 2025). Moreover, it was recently reported that branching could be repressed in Arabidopsis *clamt* mutants by engineering plants to produce 5-deoxystrigol (5DS) using *GaCYP722C* from cotton (Mizutori *et al.*, 2025). However, mutants engineered to produce 18-oxo-CLA (using *SlCYP722C* from tomato) or 4DO (using *Os900* from rice) did not show branching repression (Mizutori *et al.*, 2025). This suggests that 5DS can be an endogenous branching inhibitor, in addition to the CLAMT-LBO pathway.

ACCEPTED MANUSCRIPT

Downloaded from https://academic.oup.com/jxb/advance-article/doi/10.1093/jxb/eraf285/8174788 by guest on 10 July 2025

Further research into the CLAMT-LBO pathway may help identify branching-specific SLs and discover how they relate to exuded SLs and other plant traits. Arabidopsis lacks the complexity in SL production and exudates required to fully understand LBO function (Mizutori *et al.*, 2025). Although barley is a critical part of international grain production, relatively little is known about barley SL biosynthesis. We recently detected 6-*epi*-heliolactone, barleylactone 1 and barleylactone 2 in root exudates (Inoue *et al.*, 2024), which allowed us to test whether CLAMT-LBO is involved in the production these SLs. LBO is only a single gene in most species with one known catalytic action on MeCLA (Brewer *et al.*, 2016; Yoneyama *et al.*, 2020a; Zhou *et al.*, 2025). By contrast, CLAMT enzymes are more diverse in phylogeny and can contribute to the production of both tillering and exudate SLs (Kuijer *et al.*, 2024; Li *et al.*, 2023; Wakabayashi *et al.*, 2021). Therefore, we decided to firstly target *HvLBO* and generated a range of barley *hvlbo* mutants by TILLING and gene editing. Intriguingly, the resultant mutants displayed hallmark phenotypes that suggest a lack of SL production specific for branching. However, the mutants still produced exuded root SLs and showed no obvious defect in fungal symbiosis. These data support a model whereby (1) the LBO pathway produces branching SLs, (2) exuded SLs are produced via a split in the SL pathway upstream of LBO, and (3) exuded SLs do not normally inhibit branching.

We attempted to discover a branching SL in *hvlbo* mutants shoot tissue. However, we could not yet identify a missing SL. We previously showed in Arabidopsis that the product of LBO was poorly mobile over a graft (Brewer *et al.*, 2016). Hence, the branching influence of LBO likely breaks down quickly in tissue extracts. Further

ACCEPTED MANUSCRIPT

Downloaded from https://academic.oup.com/jxb/advance-article/doi/10.1093/jxb/eraf285/8174788 by guest on 10 July 2025

research is required to discover this branching SL and to determine why the root-exuded SLs in *hvlbo* are not involved in internal branching inhibition.

Materials and Methods

Plant materials

For work at the University of Milan, seeds of the *Arabidopsis thaliana lbo-1* mutant line (Ws-4 ecotype; T-DNA insertional mutant; code 119G09 (DYK9)) and the corresponding wild type background (Ws-4, code 530AV) were acquired from the French National Institute for Agricultural Research (INRA). Barley *lbo.f* homozygous mutants in Sebastian background and Sebastian wild-type (WT) seeds originated from University of Silesia in Katowice stocks (see below). For the production of gene edited *hvlbo* alleles at The University of Adelaide, Golden Promise was acquired from University seed stocks.

Screening for mutants in the *hvlbo* gene using the *Hor*TILLUS TILLING population

To isolate mutants carrying point mutations in the *HvLBO* gene a TILLING (Targeting Induced Local Lesions IN Genomes) strategy was used. The procedure was carried out on the population developed at the University of Silesia in Katowice, Poland called *Hor*TILLUS (*Hor*deum *vulgare* TILLING University of Silesia), which was created by double treatment of spring barley variety Sebastian with two chemical mutagens: sodium azide (NaN_3) and N-Methyl-N-nitrosourea (MNU) (Szurman-Zubrzycka *et al.*, 2018). DNA extracted from nearly 7000 M_2 individuals from the *Hor*TILLUS population

ACCEPTED MANUSCRIPT

Downloaded from https://academic.oup.com/jxb/advance-article/doi/10.1093/jxb/eraf285/8174788 by guest on 10 July 2025

was combined into eight-fold DNA pools and screened for the presence of mutations in a gene fragment encompassing the LBO catalytic domain, using the following primer pair, forward 5'-ACGAGATGGAGAGGTTGTCG-3', labelled with IRD800 dye and reverse 5'-CGATCAACTTCAGTGTGTTTTG-3', labelled with IRD700 dye. The primers were anchored in the second exon of the *HvLBO* gene. The protocol for TILLING analysis followed previous recommendations (Szurman-Zubrzycka *et al.*, 2017). Briefly, the target amplicons was generated using eight-fold pools of DNAs from M_2 individuals, using a 20 µl PCR mixture contacting 5 pmol of each primer, 0.2 mM of each of dNTP, 1 U of Color Taq DNA polymerase (EurX, Gdansk, Poland), 150 ng of template DNA and 1 x PCR buffer containing 1.5 mM $MgCl_2$. The PCR reaction profile was as follows: 3 min at 95°C, 8 cycles of touch-down with denaturation at 95°C for 30 s, annealing at 64°C for 50 s (decreasing 0.5°C per cycle) and amplification at 72°C for 1 min 30 s, followed by 30 cycles with denaturation at 95°C for 30 s, annealing at 60°C for 50 s and amplification at 72°C for 1 min 30 s. The reaction was completed by final amplification step of 5 min at 72°C. Next, the heteroduplex formation step was performed at 95°C for 3 min for initial denaturation, followed by slow renaturation in a touchdown type of reaction (70 cycles of 20 sec starting from 70°C with 0.1°C decrease per cycle). Then, the samples were treated for 15 min at 45°C with 20 µl of 0.1× Celery Juice Extract (CJE) containing Cel I enzyme that specifically cuts DNA mismatches. The products of cleavage were analyzed using polyacrylamide gel electrophoresis on LI-COR 4300 DNA Analyzer. Gel images were manually screened to detect the signals indicating putative mutations in the eight-fold DNA pools. The identification of single plants carrying the mutations was done by mixing equal amounts of DNA from each of M_2 plants that

ACCEPTED MANUSCRIPT

Downloaded from https://academic.oup.com/jxb/advance-article/doi/10.1093/jxb/eraf285/8174788 by guest on 10 July 2025

composed the specific pool with DNA from parent variety Sebastian. Such mixtures were then analyzed using the same protocol as described for the eight-fold DNA pools. All putative mutations were confirmed by Sanger sequencing.

Isolation of *hvlbo* gene edited mutant alleles

Construction of pY-LCRISPR-HvLBO was conducted following a prior protocol (Ma *et al*., 2015), including the thermocycler setups and Golden Gate assembly reactions (GGA), unless otherwise stated. The construct targeted two positions, one in exon1, HvLBO-Target-1: GAAGCTCAGGAGAGCCTGCG***AGG*** (PAM sequences bold and italic), and one in exon2, HvLBO-Target-2: CGGGTAGAAGTTCATCCGCA***CGG*** and was driven by OsU6a promoter and OsU6b promoter, respectively. Phusion® High-Fidelity DNA Polymerase (NEB) was used for all PCR reaction during plasmid construction. Overlapping PCR was used to introduce the target sequence into sgRNA cassette. All PCR fragments were confirmed by Sanger sequencing prior to use. Following sequence verification to confirm successful introduction of target sequence 1 and 2, both verified fragments were combined with binary vector pYLCRISPR/Cas9Pubi-H in a GGA reaction. For 10 µl reaction, ~40 ng of pYLCRISPR/Cas9Pubi-H plasmid was combined with ~10 ng of each sgRNA cassette fragment (7:1 vector:insert ratio), 1 unit of BsaI-HFv2 (NEB) in 1X T4 ligase buffer (NEB). The reaction was incubated at 37°C for 3 min and 16°C for 4 min (30 cycles) followed by 5 min at 60°C for enzyme inactivation. 2 µl of the reaction was transformed into 20 µl of *E. coli* TOP10 competent cells. Transformants were selected on LB media plates containing 50 µg.ml^{-1}. Prior to transformation into *Agrobacterium* AGL1, the

ACCEPTED MANUSCRIPT

Downloaded from https://academic.oup.com/jxb/advance-article/doi/10.1093/jxb/eraf285/8174788 by guest on 10 July 2025

resulting plasmid, pYLCRISPR-HvLBO, was verified using restriction enzymes and Sanger sequencing using the M13F primer 5'-TGTAAAACGACGGCCAGT-3'. The construct was transformed into immature embryos (Harwood, 2014). Following transgenic plant regeneration, transformants were screened for successful edits using PCR and Sanger sequencing of PCR products overlapping the regions using primers for Target 1: LBO-T1-F 5'-CTGACCTCGGCGGAGTACCT-3' and LBO-T1-R 5'-TTGTGAAGATCGGGCGGGTG-3' and Target 2: LBO-T2-F 5'-TTGTACCTGCCGTTGGTGAG-3' and LBO-T2-R 5'-CCACGCCTTCGTCTTCTCCG-3'. Only HvLBO-Target-1 was successful to generate *hvlbo* mutants.

HvLBO and *hvlbo.f* complementation test in the Arabidopsis *atlbo-1* mutant

To obtain the *HvLBO* CDS, gene expression in different tissues and developmental stages was analyzed mining publicly available transcriptomic data through the IPK website (https://apex.ipk-gatersleben.de/apex/f?p=284:10). The seedling stage was chosen for RNA extraction because of the early *HvLBO* expression. To clone *HvLBO* and *hvlbo.f* CDSs, RNA was extracted by Trizol protocol (Invitrogen®) from root samples of 8 day old WT Sebastian and *hvlbo.f* homozygous mutant seedlings. After DNAse I treatment and LiCl purification, reverse transcription was performed by the SUPERSCRIPT III Reverse-Transcriptase (Invitrogen®) according to the manufacturer's protocol. The CDS was amplified with high-fidelity Platinum SuperFi II DNA Polymerase (Invitrogen®) by specific tailed primers, AK365108 FW 5'-GGGGACAAGTTTGTACAAAAAAGCAGGCTATGGCTTCTGCGGCCGTCTG-3' and AK365108 RV 5'-

ACCEPTED MANUSCRIPT

Downloaded from https://academic.oup.com/jxb/advance-article/doi/10.1093/jxb/eraf285/8174788 by guest on 10 July 2025

GGGGACCACTTTGTACAAGAAAGCTGGGTCTAGTTGATCTTGGCGAAGTCCAG-3', and cloned by Gateway reaction in the p221 pDONR and pH2GW7 pDEST containing the 35S Cauliflower Mosaic Virus (CaMV) promoter and terminator.

Agrobacterium tumefaciens GV3101 was used to transform *atlbo-1* homozygous mutants by floral dip (Clough and Bent, 1998). T1 seeds were screened on hygromycin selective media and resistant seedlings were checked for transgene presence by PCR employing primers HvLBO/hvlbo.f FW 5'-CGAGATGGAGAGGTTGTCGA-3' and HvLBO/hvlbo.f RV 5'-GTCTTCTTGCCCTCGAGCTT-3'. Transgene expression was assessed by qRT-PCR. To test expression in transgenic Arabidopsis plants, RNA was extracted from rosette leaves using the LiCl method (Verwoerd *et al.*, 1989). After DNAse treatment, for each sample, RNA was retro-transcribed using iScript kit (BioRad). qRT-PCR assay was performed using iTaq Universal SYBR Green supermix (BioRad) in a Bio-Rad iCycler iQ Optical System (software version 3.0a). Relative transcript enrichment of the targets of interest was calculated by normalizing the amount of mRNA against the ubiquitin-like *RCE1* transcript (At4g36800) (Pribil *et al.*, 2010) and the *EIF4* transcript (At3g13920) (Yamaguchi *et al.*, 2009). Expression of the genes was calculated using the $2^{-\Delta\Delta Ct}$ method, employing WT as the normalizer. The primers used for qPCR were HvLBO-SEED1 5'-TCTTCTCCGAAGACCAGAAGC-3', HvLBO-SEED2 5'-CTCGGCGGAGTACCTTTCC-3' used to evaluate the expression level of both *HvLBO* and *hvlbo.f* transcript, and RCE1-147 5'-CTGTTCACGGAACCCAATTC-3' and RCE1-148 5'-GGAAAAAGGTCTGACCGACA-3' for *RCE1* transcript, and RT2414 5'-AAACTCAATGAAGTACTTGAGGGACA-3' and RT2415 5'-

ACCEPTED MANUSCRIPT

Downloaded from https://academic.oup.com/jxb/advance-article/doi/10.1093/jxb/eraf285/8174788 by guest on 10 July 2025

TCTCAAAACCATAAGCATAAATACCC-3' for *EIF4* transcript. T2 and T3 seeds were selected on hygromycin media in order to track plants bearing the transgene in homozygosity or with copy number that does not give WT segregation in up to 40 T3 plants. Those T3 seeds were used for the phenotypic analysis and three plants of each T3 line were checked for transgene expression and silencing.

Plant treatments and phenotypic analyses

Arabidopsis seeds were sown in multipot plateaus (2.5 cm diameter each pot) and stratified in soil for 2 days. Plants were grown in SD condition (8h day/16h night, 20-22 °C) for 14 days and then moved to LD (16h day/8h night, 20-22 °C). The SD condition was used to delay flowering and increase rosette leaf production and branching. As near as possible to the first senescent silique, the number of rosette branches bigger than 5 mm was counted (Brewer *et al.*, 2016). 25-27 plants per genotype were used and grown in a partially block-randomized setting.

A greenhouse experiment (2019-2020) was set up to phenotype barley *Hor*TILLUS lines carrying point mutations in *hvlbo* (Table 1) and WT cultivar Sebastian, following a random block design, with 19 incomplete blocks. In the final design we included 27 Sebastian plants and 19 *hvlbo.f* plants. Seeds were sterilized for 1 min in 1% sodium hypochlorite, rinsed in water once, then 2 min in 70% ethanol, and rinse three times in water. Seeds were then sown on a rooting medium containing 2.15 g L^{-1} Murashige and Skoog salts with vitamins (Duchefa Biochemie), 30 g L^{-1} sucrose, 8 g L^{-1} plant agar (Duchefa Biochemie), and 5 mL L^{-1} indole-3-butyric acid (IBA; 0.1 mg mL^{-1} stock)

ACCEPTED MANUSCRIPT

Downloaded from https://academic.oup.com/jxb/advance-article/doi/10.1093/jxb/eraf285/8174788 by guest on 10 July 2025

(Sparkes *et al.*, 2006) and incubated in a growth room in the dark at 24C°. When they reached one-leaf stage, seedlings were transplanted in soil in 14x14x16 cm pots (one plant per pot) and grown in a greenhouse at Orto Botanico Città Studi, located in Via Camillo Golgi 18 in Milan, under long day photoperiod (16 hours light at 20°C and 8 h dark at 17°C), 60-65% humidity, 200 µE m^{-2} s^{-1} light. The number of tillers at different days after sowing (DAS) was recorded for each plant, along with plant height (distance between the point of emergence from the soil and the base of the spike) and tiller number at harvest stage.

Gene edited alleles were developed and assessed in a glasshouse under long days (16/8 h) at 21/16°C with daylight supplemented with 400W Metal Halide lamps (Plusrite) at the South Australia Research & Development Institute (SARDI) Plant Research Centre, University of Adelaide Waite Campus. Plants were grown in SARDI's proprietary Cocopeat soil mix, containing 56% coir fibre, 44% quarried drainage sand and controlled release fertilizer (N added separately) at 2 cm sowing depth in 17.5 cm diameter, 11.6 cm height, 2.8 L pots with calcium nitrate watered in at the start at the specified rates. Hormone treatments contained either 2 µM GR24 (*rac*-GR24, PhytoTech Labs, G3324) or mock without hormone addition. Treatment solutions contained one drop of Triton X surfactant and 10 µL acetone (GR24 was dissolved in acetone) per 50 mL MilliQ water. Hormone solutions were applied to tiller buds under the leaf sheaths using a pipette starting from mid-tillering phase (Zadok stage 24). Treatments were applied 3 times per week (Mon, Wed, Fri) over a 6-week period. 200 µL of solution was applied for early development, increasing to 400 µL, 800 µL and

ACCEPTED MANUSCRIPT

Downloaded from https://academic.oup.com/jxb/advance-article/doi/10.1093/jxb/eraf285/8174788 by guest on 10 July 2025

1200 µL as plant size progressively increased. Tiller number was manually scored at the end of development.

For hydroponic experiments in Japan, barley plants were assessed in half-strength Tadano and Tanaka (TT) (Tadano and Tanaka, 1980) liquid culture using our reported plastic cup hydroponic method (Yoneyama *et al.*, 2020b) and including the specified nutrient restrictions.

SL collection from root tissues and exudates and LC-MS/MS

SLs were collected and analyzed following our reported methods for root tissues and exudates (Inoue *et al.*, 2024; Yoneyama *et al.*, 2022). Barley SLs were analyzed using ultra performance liquid chromatography coupled to tandem mass spectrometry (UPLC-MS/MS). For this, the Acquity UPLC System (Waters) coupled to a Xevo TQD triple-quadrupole mass spectrometer (Waters MS Technologies) with electrospray (ESI) interface was used. Chromatographic separation was achieved using an ODS column (ACQUITY UPLC, BEH C18, 2.1 × 100 mm, 1.7 µm; Waters) with a water-MeOH gradient containing 4% 50 mM ammonium acetate to promote ionization. Separation started at 35% MeOH, followed by a 2 min gradient to 55% MeOH, followed by a 13 min gradient to 95%, kept 96% MeOH for 2 min to wash column and then back to 35% MeOH for 3 min. The column was equilibrated at this solvent composition for 5 min before the next run. Total run time was 25 min. The column oven temperature was maintained at 40°C with a flow-rate of 0.2 mL min^{-1} (sample injection volume of 1 µL). MRM transitions for 6-*epi*-heliolactone eluting at 5.5 min were monitored for m/z 361/97

ACCEPTED MANUSCRIPT

Downloaded from https://academic.oup.com/jxb/advance-article/doi/10.1093/jxb/eraf285/8174788 by guest on 10 July 2025

at a collision energy (CE) of 18 V and m/z 361/233 at CE of 18 V with a cone voltage of 25 V. The MRM transitions of m/z 377/97 at CE of 20 V and m/z 377/231 at CE of 15 V with a cone voltage of 25 V were used for the detection of barleylactone 2 (a novel epoxy variant of 6-*epi*-heliolactone) eluting at 4.4 min. SLs are inherently low-abundance molecules that are difficult to precisely measure, hence we could only determine relative levels ("peak areas") between samples rather than absolute concentrations.

Arbuscular mycorrhizal fungi colonization assay

Arbuscular mycorrhizal (AM) fungi colonization assays were carried out at the Adelaide SARDI facilities using a clay loam that was dried and then sieved to <2 mm. A fine sand and the sieved soil were then sterilized by autoclaving at 121°C for 20 min, two times with >24 hours between autoclave runs. Free-draining, 0.8L plastic pots were used, and each pot held 1.1 kg of the soil mix (loam soil:dry sand, 1:1). Soil and sand were homogenously mixed prior to potting. The AM treatment was inoculated with four isolates of the AM fungus *Rhizophagus irregularis* as a commercial product (Start Up Ultra, Microbe Smart Pty Ltd, Australia) at a rate of 1 g kg^{-1} soil (corresponding to approximately 800 spores pot^{-1}) and then mixed thoroughly with the soil. The non-AM control pots had no inoculum mixed with the soil. For AM fungus un-inoculated (-AMF) treatment, there were 6 pots prepared for each genotype (GP WT, *Ibo-2* and *Ibo-3*). For AM fungus inoculated (+AMF), there were 10 pots prepared for each genotype, where 6 pots were for the main experiment and 4 extra pots were prepared for mid-experiment destructive sampling. 3-4 seeds were directly sown onto the soils. Plants were watered

ACCEPTED MANUSCRIPT

Downloaded from https://academic.oup.com/jxb/advance-article/doi/10.1093/jxb/eraf285/8174788 by guest on 10 July 2025

approximately every two days with 50 mL water. Pots with more than 3-4 seedlings emerged were thinned to 2 seedlings, 14 days after sowing. At 48 days after planting, plants were gently removed from the soil and any roots with attached soil were washed clean. A representative sub-sample of fresh roots (approx. 200 mg) was taken and placed in a tissue cassette, submerged in 50% ethanol for at least 24 hours to fix. The fresh root subsamples were subsequently rinsed and placed into 10% potassium hydroxide (KOH) (w/v) solution for clearing at room temperature for seven days. Then, the samples were rinsed well and stained in a 5% ink in vinegar solution (Vierheilig *et al.*, 1998) and then de-stained in acidified RO water for at least 24 hours, before being stored in a 50% glycerol solution. The roots were then quantified for percentage root length colonized by AM fungi under a stereomicroscope using the gridline intersect method (Giovannetti and Mosse, 1980).

Parasitic weed seed germination bioassay

2.5 mL of each exudate collected sample was concentrated and applied to seeds of branched broomrape (*Phelipanche ramosa*) and Egyptian broomrape (*Phelipanche aegyptiaca*), and assessed for percentage germination, according to our published method (Inoue *et al.*, 2024).

Data analysis

Data obtained from the above experiments were obtained via manual collection and were arranged in Microsoft Excel. All data was transferred to GraphPad Prism for statistical analysis and visualization. Comparisons between 2 groups used parametric *t*-

ACCEPTED MANUSCRIPT

Downloaded from https://academic.oup.com/jxb/advance-article/doi/10.1093/jxb/eraf285/8174788 by guest on 10 July 2025

tests to determine statistical relationships. For multiple comparison tests between more than 2 groups, one-way and two-way ANOVA with Tukey *post hoc* tests were used to determine statistical relationships.

Results

Barley *HvLBO* shows functional conservation in *Arabidopsis thaliana*

Sequence searches using Arabidopsis *AtLBO* At3g21420 identified a single barley gene (HORVU.MOREX.r3.3HG0314210) in the Morex V3 reference genome (Mascher *et al.*, 2021), encoding a protein of 375 amino acids with high similarity to proteins from related species, rice, *Brachypodium distachyon* and sorghum, and to Arabidopsis AtLBO (59% identity, 77% similarity) (Supplementary Fig. S1). The sequence contains within exon 2 a conserved double-stranded β-helix conserved catalytic domain (DSBH), which is a hallmark of 2-OGDs (Fig. 1A). We previously showed that the enzymatic activity of this protein was the same whether it came from tomato, maize, sorghum or Arabidopsis (Yoneyama *et al.*, 2020a). To validate functional orthology of this candidate *HvLBO* from barley, an interspecific complementation of the Arabidopsis *atlbo-1* mutant was employed. Whereas *atlbo-1* showed increased branching (Brewer *et al.*, 2016), 35S-driven constitutive expression of *HvLBO* CDS in the Arabidopsis mutant fully restored branching to WT (Ws-4) levels in four independent lines (Fig.1B). This confirms functional conservation of *LBO* across monocotyledonous and dicotyledonous plants. Expression of *HvLBO* in Arabidopsis did not inhibit branching below WT levels (Fig. 1C). However, high SL production would be expected to repress the endogenous SL pathway in Arabidopsis as a form of feedback (Hellens *et al.*, 2023).

ACCEPTED MANUSCRIPT

Downloaded from https://academic.oup.com/jxb/advance-article/doi/10.1093/jxb/eraf285/8174788 by guest on 10 July 2025

Barley *hvlbo* mutants display a sub-set of SL phenotypes

We employed TILLING using the *Hor*TILLUS mutagenized population of two-row spring barley (*Hordeum vulgare* L. cv. 'Sebastian') (Szurman-Zubrzycka *et al.*, 2018) to find potential *hvlbo* mutant alleles. Screening of 6912 M_2 plants resulted in the identification of 12 lines harboring distinctive point mutations in the target gene. Out of these, four lines carrying independent missense mutations (Table 1) showed viable seed germination and were further examined under glasshouse conditions. All mutations in these *hvlbo* alleles fell within the putative LBO catalytic domain near the C-terminus. One allele in particular, *hvlbo.f*, contained a point mutation in the coding sequence at G845A, which would result in residue change D251N (Supplementary Fig. S1; Fig. 1A). Residue 251 is a conserved aspartic acid (D) residue that is predicted to play a critical role in iron binding within the LBO catalytic domain (Brewer *et al.*, 2016). Thus, this mutation is predicted to significantly interrupt lbo enzymatic function, and we analyzed this line further. Consequently, the *hvlbo.f* line exhibited increased tiller number at harvest compared to WT Sebastian (Fig. 1D) and reduced plant height (Fig. 1E), similar to SL-defective phenotypes reported in rice and other species (Gomez-Roldan *et al.*, 2008; Umehara *et al.*, 2008). Tiller number reached a plateau 64-70 days after sowing in the WT, but continued to increase for a further two weeks in the *hvlbo.f* line (Fig. 1D).

To validate these results, a construct expressing the *hvlbo.f* CDS under the control of the 35S CaMV constitutive promoter was introduced in the Arabidopsis *atlbo-1* mutant and branch number (Fig. 1F) and the relative expression of the transgene was evaluated in T3 lines (Fig. 1G). According to the phenotype of four T3 independent lines, *hvlbo.f* was not able to fully complement the *atlbo-1* branching phenotype in any of the analyzed lines. Indeed, we detected

ACCEPTED MANUSCRIPT

Downloaded from https://academic.oup.com/jxb/advance-article/doi/10.1093/jxb/eraf285/8174788 by guest on 10 July 2025

a partial complementation only in two out of the four analyzed lines (Fig. 1F). These results suggest only a partial functionality of the *lbo.f* allele.

Further barley mutant alleles were generated by targeting exon 1 and exon 2 of *HvLBO* with a CRISPR-Cas9 site-directed nuclease construct transformed into barley (*Hordeum vulgare* L. cv. 'Golden Promise'). Two new alleles, *hvlbo-2* and *hvlbo-3*, were identified that carry single base changes resulting in frame-shifts early in the coding sequence, which would result in severe protein truncation and loss of the catalytic domain (Fig. 1A). We grew *hvlbo-2* and *hvlbo-3* mutants individually in hydroponic cups and compared plants to *hvd14.d*, a previously isolated mutant in the SL receptor gene (Marzec *et al.*, 2020a; Marzec *et al.*, 2016). The *hvlbo* mutants showed increased tillers (Fig. 2A-C). Mutant plants of *hvd14* showed on average 2.2 (± 0.4) extra tillers at 18 days old compared to the WT variety (*Hordeum vulgare* L. cv. 'Sebastian'), while *hvlbo-2* and *hvlbo-3* showed 1.3 (± 0.3) and 1.6 (± 0.5) extra tillers respectively, compared to Golden Promise (Fig. 2B). Plants in hydroponic cups have a limited lifespan and can experience some stress, which may affect tillering. Hence, we examined other plants grown individually in pots with normal soil and nutrients. Analysis of tiller number over time revealed that *hvlbo-2* mutant tiller numbers were not significantly different during early growth compared to WT (Golden Promise), but *hvlbo-2* ended up with more tillers (Fig. 2C), consistent with results obtained with *hvlbo.f* (Fig. 1D). This confirms that SLs are more important for tiller repression in older plants. Further experiments are required to understand whether this represents a direct effect on older tiller bud outgrowth.

Other individual plants were grown in hydroponic cups and transferred at 18 days into phosphorus (P) starvation conditions to boost SL production. At 28 days, the root tissues were extracted and assessed for any SLs. 6-*epi*-heliolactone and barleylactone 2 (a novel epoxy variant of 6-*epi*-heliolactone) have recently been detected as predominant SLs in barley (Inoue

ACCEPTED MANUSCRIPT

Downloaded from https://academic.oup.com/jxb/advance-article/doi/10.1093/jxb/eraf285/8174788 by guest on 10 July 2025

et al., 2024). We also detected these SLs in root tissues in all genotypes (Fig. 2D, E). Surprisingly, the peak areas of the mass spectrum were all very similar, including from *hvlbo-2* and *hvlbo-3*, indicating similar levels of SL production, regardless of the genetics (Supplementary Fig. S2; Fig. 2D, E). Root biomass was not greatly different, suggesting that root growth is not a compounding factor that may affect SL production (Fig. 2F). Similar SL levels in WT and *lbo* mutants suggests that LBO is not required for 6-*epi*-heliolactone and barleylactone 2 production within roots. Lack of SL signaling in *d14* might be expected to increase SL production due to feedback (Arite *et al.*, 2009). However, we did not see increased SL in *hvd14.d*, which may indicate a lack of *D14*-dependent feedback in barley (at least for 6-*epi*-heliolactone and barleylactone 2 content within roots).

Barley *hvlbo* mutant tiller number is greater and less reactive to nutrient conditions

As noted above, nutrients can repress SL production, and P or nitrogen (N) starvation is a common way to boost SL production for research (Brewer *et al.*, 2013). Nutrients promote the number of grain-bearing shoots (branches/tillers), which enables plants to increase progeny in proportion to greater resource availability (Brewer *et al.*, 2013). Hence, fertilizer can increase yield in crops by boosting the number of tillers. Conversely, this relationship can have adverse effects on final tiller number and yield if growers seek to reduce fertilizer use (Francis *et al.*, 2023; Kelly *et al.*, 2023). SL biosynthesis gene expression, including *LBO*, can also be highly suppressed by N (Lailheugue *et al.*, 2023). We supposed that LBO, as a key SL enzyme, would also be part of nutrient responses in barley. Hence, we examined *hvlbo-2* in more detail. Plants were grown in pots in soil with low, intermediate and normal N levels and phenotypic changes were examined. Mutant *hvlbo-2* plants consistently displayed greater tiller numbers than the WT control variety (Golden Promise) (Fig. 3A). Tiller number aligned well with grain number (Fig.

ACCEPTED MANUSCRIPT

Downloaded from https://academic.oup.com/jxb/advance-article/doi/10.1093/jxb/eraf285/8174788 by guest on 10 July 2025

3B) and yield per plant (Fig. 3C), and inversely with average individual grain (kernel) mass (Fig 3D). In each case, WT response to N was greater than *hvlbo-2* and tended to converge with the mutant at higher N. This aligns with the known role of SLs in adapting crop plants to nutrient levels (Brewer *et al.*, 2013; Huang *et al.*, 2025; Sigalas *et al.*, 2024). Mutant and WT phenotypes tend to converge in high N, because the SL pathway becomes suppressed by N in the WT (Sun *et al.*, 2023; Wu *et al.*, 2020). Hence, under optimal conditions, SL levels in the WT and mutant plants are similarly low and the plants appear more similar in phenotype.

Barley *hvlbo* mutants retain yield and fertility at low N, but produced grains of reduced mass

Interestingly, *hvlbo-2* showed 29% greater yield than WT at 250 mg/kg N (Fig. 3C). Harvest index (Fig. 3E) and seed set (Fig. 3F) were also higher at 250 mg/kg N. This means that, in WT, SLs produced by LBO contribute to a repressive effect on yield, harvest index and fertility in low N, because these inhibitions were not as strong in the mutant. Hence, mutant variants of *lbo* may be useful in breeding to prevent yield loss from poorly fertile soil or low fertilizer use. On the other hand, yield was 13% lower in *hvlbo-2* at 750 mg/kg N. This was mostly due to lower individual grain mass that offset increased tiller and grain number. Smaller grain size has been observed in SL mutants in rice and maize (Guan *et al.*, 2023; Yamada *et al.*, 2019). This implies that SLs produced by LBO in the WT help plants to maintain the high mass of individual grains, even if grain number increases. Hence, LBO-related SLs may have positive or negative effects on yield and grain mass, depending on the conditions. Shoot biomass (Fig. 3G) and plant height (Fig. 3H) were only slightly different, indicating that the mutants did not show a strong growth or stature defect, which might otherwise repress grain mass. Likewise, root biomass was not greatly different in various experiments (Fig. 2F and see below).

ACCEPTED MANUSCRIPT

Downloaded from https://academic.oup.com/jxb/advance-article/doi/10.1093/jxb/eraf285/8174788 by guest on 10 July 2025

Barley *hvlbo* responded to SL treatment, but showed normal root fungal symbiosis

To further test *hvlbo* mutants, we added a synthetic SL (*rac*-GR24) to *hvlbo-2* mutants and observed that tiller number was repressed to near the level of WT (Fig. 4A). This suggests that barley tiller buds are responsive to SLs and that *hvlbo* mutants are deficient in the production of a branching inhibiting SL. SL branching repression below control WT was not observed. SL feedback homeostasis, whereby SLs repress SL biosynthesis, is proposed to explain resistance to exogenous SLs in WT (Dun *et al.*, 2023). The lack of increased SL production in *hvd14.d* roots (Fig. 2D, E) may contradict that, but autoregulation of the signaling complex may also provide SL resistance (Dun *et al.*, 2023).

We also examined the capacity for arbuscular mycorrhizal (AM) fungal colonization in *hvlbo-2* and *hvlbo-3* mutant roots at 48 days post inoculation (dpi). Hyphae, vesicles and arbuscules were observed in roots, indicating that colonization had occurred. However, no significant differences were observed between mutants and WT in terms of overall colonization and fungal morphology (Fig. 4B). In addition, we confirmed no change in AM fungal colonization in *hvlbo-2* and *hvlbo-3* in an independent laboratory using alternative inoculation and scoring methods (Supplementary Fig. S3 and Supplementary Protocol S1). AM fungal colonization coincided with slightly repressed root and shoot biomass at 34 dpi (Fig. 4C, D). This result may indicate a carbon drain, negatively affecting plant growth, as has been reported in barley previously (Grace *et al.*, 2009; Kaur *et al.*, 2022). Importantly, similar biomass reduction trends were seen across WT, *hvlbo-2* and *hvlbo-3* (Fig. 4C, D), suggesting that the fungal interaction is functioning in a similar way in the mutant and WT. Root biomass was slightly reduced compared to the WT in *hvlbo-2* and *hvlbo-3*, and the shoot biomass trended slightly higher, which suggests that the *LBO* pathway may play a minor role in balancing root and shoot growth, in a manner

ACCEPTED MANUSCRIPT

Downloaded from https://academic.oup.com/jxb/advance-article/doi/10.1093/jxb/eraf285/8174788 by guest on 10 July 2025

unrelated to AM fungal colonization. A thorough examination of *hvlbo* root architecture responses to nutrients would be useful for future studies.

Barley *hvlbo* mutants have normal SL root exudates

Having established that *lbo* mutant plants show phenotypes that align with SL deficiency, and yet show normal SL production in root tissues, and no obvious signs of deficient AM fungal symbiosis activity, we next sought to test whether exuded SL was defective in mutants. We grew *hvlbo-2* mutant plants in P- and N-deficient conditions to boost SL production, and the SLs exuded from roots were collected and analyzed by liquid chromatography with tandem mass spectrometry (LC-MS/MS). We detected and identified the same two SLs (Fig. 2D, E): 6-*epi*-heliolactone and barleylactone 2 (Supplementary Fig. S4; Fig. 5A, B). As expected, SL secretion greatly increased in the WT: 6-*epi*-heliolactone (Fig. 5A) and barleylactone 2 (Fig. 5B). This was especially so for N deficiency. Remarkably, *hvlbo-2* mutants showed very similar increases. Parasitic weed seed germination is a reliable bioassay used to verify that bioactive SLs are present in a sample, particularly when SL levels are near the limit of detection (Ablazov *et al.*, 2024). The WT and mutant collected exudate stimulated parasitic weed seed germination with trends matching the SL detection data (Fig. 5C, D), confirming similarity of SL levels. This implies that the product of LBO is not an important contributor to SL exudate production.

Discussion

Until recently, all reported SL mutants were highly branched. Also, SLs can inhibit buds when applied exogenously, and there usually exists only one copy of the SL receptor in a species. Hence, it had been assumed that all SLs produced within plants will inhibit buds. However, research into the sub-pathway of SL biosynthesis that involves CLAMT and LBO, along with new SL biosynthesis mutants that are not highly branched, suggest that there may be (at least)

ACCEPTED MANUSCRIPT

Downloaded from https://academic.oup.com/jxb/advance-article/doi/10.1093/jxb/eraf285/8174788 by guest on 10 July 2025

exudate- and branching-specific SL pathways (Chen *et al.*, 2023; Ito *et al.*, 2022; Li *et al.*, 2023; Wakabayashi *et al.*, 2019; Wang *et al.*, 2024). This may mean that, despite years of research into branching and SLs, the branching-specific SL is yet unknown (Dun *et al.*, 2023; Nomura *et al.*, 2024; Yoneyama and Brewer, 2021). Therefore, it is useful to discover whether *lbo* mutants are defective in exuded SLs. In this study, we show that *lbo* mutants in barley fail to produce the SL-related branching inhibitor, but are still able to make exuded SLs.

Exudate SLs may include various structures, including four-ringed types (canonical) and non-four-ringed types (non-canonical). The production of known canonical SLs mostly involves consecutive reactions from P450 enzymes deriving from carlactonoic acid (CLA), a non-bioactive, two-ringed SL intermediate (Dun *et al.*, 2023). Plant species and varieties can exude their own distinctive mix of SLs. This is presumably to avoid parasitic weed infection but still retain AM fungal interactions (Yoneyama and Brewer, 2021). It is not yet well known how the diversity in exuded SLs relates to internal hormone function and evolution. Branching-specific SLs are likely to be CLA-derived and non-canonical. Methyl carlactonoate (MeCLA) is produced from CLA by the CLAMT enzyme (Haider *et al.*, 2023; Li *et al.*, 2023; Mashiguchi *et al.*, 2022; Wakabayashi *et al.*, 2021) and MeCLA is a precursor for non-canonical SLs (so far). MeCLA was shown to be the precursor to lotuslactone, zealactone or avenaol, all found in root exudates (Dun *et al.*, 2023; Yoneyama and Brewer, 2021). LBO is a 2-OGD enzyme that acts to convert MeCLA into hydroxymethyl carlactonoate (1'-HO-MeCLA), a function that appears to be conserved in monocotyledonous and dicotyledonous plants (Brewer *et al.*, 2016; Yoneyama *et al.*, 2020a). Mutants of *clamt* or *lbo* in Arabidopsis show increased branching, suggesting that this pathway produces a branching inhibiting SL (Brewer *et al.*, 2016; Zhou *et al.*, 2025). This also means that LBO is currently the enzyme in the most distal position in the pathway that produces the branching SL. However, the identity of that SL, or what further conversions or transport may occur, are unknown. The LBO enzyme, when heterologously expressed in

ACCEPTED MANUSCRIPT

Downloaded from https://academic.oup.com/jxb/advance-article/doi/10.1093/jxb/eraf285/8174788 by guest on 10 July 2025

Escherichia coli, produces 1'-HO-MeCLA, but it also produces CLA, and at greater levels (Yoneyama *et al.*, 2020a). Mutants of *lbo* have high levels of MeCLA and undetectable levels of 1'-HO-MeCLA (Yoneyama *et al.*, 2020a). 1'-HO-MeCLA is predicted to be unstable and CLA may be a non-enzymatic reversion from 1'-HO-MeCLA that occurs perhaps in the absence of further enzymatic processing or perception (such as would occur in *E. coli*). However, the instability of 1'-HO-MeCLA may mean it cannot be chemically synthesized for further testing. Likewise, further research into the *in planta* function of LBO remains challenging.

Meanwhile, *lbo* mutants have been so far only revealed in Arabidopsis (Brewer *et al.*, 2016; Zhou *et al.*, 2025). However, Arabidopsis seems to have a simplified SL biosynthesis pathway, perhaps because hormone function has been retained but AM fungal symbiosis has been lost during evolution. Hence, sub-pathways of SL biosynthesis relating to AM fungi appear to be also lost. Therefore, it may be useful to study *lbo* mutants in species that have the capacity to associate with AM fungi. Hence, we isolated *hvlbo* mutants in barley by TILLING and gene editing. The mutants showed the expected increased tillering phenotype of SL mutants (Fig. 1D, 2A-C, 3A, 4A), although not as strong as *hvd14* (Fig. 2B). Previously, Arabidopsis mutants of *lbo* showed intermediate branching, perhaps due to a buildup of MeCLA, which presumably is only weakly bioactive (Brewer *et al.*, 2016). It is also important to consider that SLs are not the only signal that regulates branching. Cytokinins, sugar signaling and bud auxin transport also promote tillering and still function in SL mutants (although they may be altered by complex feedback mechanisms) (Beveridge *et al.*, 1997; Salam *et al.*, 2021; Zhang *et al.*, 2020).

Mutants of *hvlbo* also showed a decrease in average individual grain mass (Fig. 3D). This is similar to rice and maize SL mutants (Guan *et al.*, 2023; Yamada *et al.*, 2019). Increased grain number in *hvlbo* was largely offset by reduced grain mass, which tended to make yield per plant similar to WT (Fig. 3C). Further research is needed to determine whether the lower grain mass

ACCEPTED MANUSCRIPT

Downloaded from https://academic.oup.com/jxb/advance-article/doi/10.1093/jxb/eraf285/8174788 by guest on 10 July 2025

in *hvlbo-2* is due to resource limitation from too many tillers or any defect directly in grain development. The latter is currently favored based on tiller removal in rice SL mutants that did not restore the smaller grain size (Yamada *et al.*, 2019). The *hvlbo* mutants had levels of two SLs in root tissues that were similar to WT and the *hvd14.d* mutant (Fig. 2D, E), yet tiller number was repressed by adding SL (Fig. 4A). This may indicate that LBO is defective in making some type of SL, but not these two. It is unclear if other SLs are made by barley. There are five *MAX1* homolog genes in barley that are partly conserved and partly divergent from the MAX1 homologs in rice (Marzec *et al.*, 2020b), so other SLs may exist. 5-deoxystrigol was previously reported for barley (Wang *et al.*, 2018), however, we could not yet detect it or any other SLs. We are currently isolating a range of SL biosynthesis mutants, which will help to elucidate the entire SL pathway in barley, and clarify the role of LBO.

The *hvlbo* mutants showed a general lack of response to nitrate, which would be expected for an SL mutant. The lack of response ultimately meant that yield was higher at low nitrate, but lower at higher nitrate (Fig. 3C). This opens up the potential to develop *lbo*-related genetic variants to employ in poorly fertile soils or when less fertilizer is used (Kelly *et al.*, 2023). Field trials will be useful to further explore this concept. In the case of barley, consistent grain size, germination and protein content is important for malting. So, grain quality analysis, such as germination and protein levels will be useful in future. A trade-off of low grain mass may not be desirable for malting barley, but may be acceptable for livestock feed. Also, because barley *hvd14* mutants were shown to be defective in drought response (Marzec *et al.*, 2020a), *hvlbo* mutants should also be assessed for this trait in future. We do not yet know exactly what traits may be regulated by the *LBO* pathway, in addition to branching and grain size. For instance, AM fungi symbiosis was not obviously affected in the mutants (Fig. 4B), but stress response is yet unknown. Plants were shorter in *hvlbo.f* (Fig. 1E) compared to *lbo-2* (Fig. 3H). Further research is needed to test whether the growth conditions, cultivar background or a second-site mutation

ACCEPTED MANUSCRIPT

Downloaded from https://academic.oup.com/jxb/advance-article/doi/10.1093/jxb/eraf285/8174788 by guest on 10 July 2025

may have specifically enhanced dwarfing in *hvlbo.f*. To date, we would not yet rule out shade avoidance as a trait regulated by *LBO*.

We observed normal SL exudation and effects in *hvlbo* mutants. AM fungi symbiosis (Fig. 4B), the production of two SLs in root tissue (Fig. 2E, F) and exudates (Fig. 5A, B), and exudate germination stimulation of parasitic weed seeds (that are extremely sensitive to SLs) (Fig. 5C, D) suggest that SL production in roots is normal in *hvlbo* mutants. SLs affect root architecture (Brewer *et al.*, 2013). The root biomass of *hvlbo* mutants was not greatly different, but it will be important to discover whether there are subtle differences. Remaining important questions are: does LBO have any role in roots, and can root SL exudate production can be separated from root architecture?

We uncovered two SLs at similar levels in WT and *hvlbo* roots and exudates. Importantly, this means that LBO is not required to produce those SLs and that those SLs are not involved in branching. 6-*epi*-heliolactone has been identified as a biosynthetic intermediate between MeCLA and avenaol in black oat (Moriyama *et al.*, 2022). Treatment with prohexadione, a 2-OGD inhibitor, repressed the conversion of 6-*epi*-heliolactone to avenaol in black oat (Moriyama *et al.*, 2022). However, our results suggest that LBO is not involved in 6-*epi*-heliolactone production, at least in barley. Another 2-OGD may produce avenaol, such as LOTUSLACTONE-DEFECTIVE (LLD), a 2-OGD involved in lotuslactone production in the legume *Lotus japonicus* (Mori *et al.*, 2020), or a yet unknown 2-OGD.

The detection of normal levels of SLs in roots and exudates in *lbo* mutant suggests that the LBO enzyme is not significantly involved in the biosynthesis or exudation, or even the feedback, of those SLs. This supports the hypothesis that LBO has specificity for branching, but not exudation. *hvlbo* mutant plants can make SLs, and those SLs are not able to significantly inhibit

ACCEPTED MANUSCRIPT

Downloaded from https://academic.oup.com/jxb/advance-article/doi/10.1093/jxb/eraf285/8174788 by guest on 10 July 2025

branching as an internal hormone. It is possible that they simply cannot travel to tissues where branching inhibition occurs. Transport can be influenced by SL structure (Xie *et al.*, 2016). It has been suggested that the hormonal function of LBO is to convert MeCLA into branching SLs close to buds (Brewer *et al.*, 2016; Dun *et al.*, 2023; Yoneyama and Brewer, 2021). Differences in chemistry may mean that CLA is a soluble transported form that is converted to MeCLA in target tissues for further processing by LBO (Dun *et al.*, 2023). Thus, specialized transport and delivery near buds may be a key specification for the branching SL and may explain why other SLs cannot functions in that way. Novel SLs are regularly being discovered, even in well-studied species. Work will continue to discover the gamut of SLs in barley, especially those particularly involved in bud outgrowth.

Acknowledgments

This article is dedicated to our esteemed colleague and mentor, the late Prof. Dabing Zhang. Thanks to Ghazwan Karem, Toby Gerard, Saffron Gerard, Mitchell Booker, Amber Walker, Ethan Habets, Breanna Forster, and Antonella Monte for technical assistance, and Elizabeth Dun for discussions

Author contributions

LR, KY, and PBB: conceptualization; AS, JHK, WC, AJ, LR, KY, and PBB: methodology; MI, AS, JHK, WC, HZ, CCF, SS, AB, SJWW, AJ, RA, BC, LR, KY, and PBB: formal analysis; MI, AS, JHK, WC, HZ, CCF, VG, AV, SS, AB, SJWW, AJ, RA, BC, LR, KY, and PBB: investigation; DZ, AJ, MM, LR, KY, and PBB: resources; LR and PBB: writing – original draft; AS, JHK, CCF, VG, MTW, MRT, SJWW, AJ, LR and PBB; writing – review and editing; KY and PBB:

ACCEPTED MANUSCRIPT

Downloaded from https://academic.oup.com/jxb/advance-article/doi/10.1093/jxb/eraf285/8174788 by guest on 10 July 2025

visualization; VG, MRT, DZ, LR, KY, and PBB: supervision; JHK, VG, DZ, AJ, MM, LR, KY, and PBB: funding acquisition.

Conflict of interest

No conflict of interest declared.

Funding statement

This research was supported by the Australian Research Council (ARC) Fellowship (FT180100081) and South Australian Grain Industry Trust grant (UAD 02023) to PBB, an ARC Discovery Project (DP24 0102441) to MTW and PBB; an Australian Government Research Training Program (RTP) Scholarship and a Thyne Reid Foundation/Playford Trust Scholarship to JHK, the ERA-NET Cofund FACCE SURPLUS (BarPLUS grant id. 93) funded by MIUR in Italy to LR and by NCBR in Poland to AJ. AR was supported by a scholarship from the Saudi Arabia Ministry of Higher Education-King Saud University. Work at University of Milan was in part supported by the CLIMBER project funded under the University's 2019 SEED call (grant number 1253 to LR and VG). LR also acknowledges financial support under the National Recovery and Resilience Plan (NRRP), Mission 4, Component 2, Investment 1.1, Call for tender No. 104 published on 2.2.2022 by the Italian Ministry of University and Research (MUR), funded by the European Union – NextGenerationEU– Project Title "RADICALS - Root and shoot developmental insights for crop agricultural traits affecting resilience, competitiveness and sustainability" – CUP G53D23004030006 - Grant Assignment Decree No. n. 1048 adopted on 14/07/2023 by the Italian Ministry of Ministry of University and Research (MUR). KY was supported by Japan Science and Technology Agency (FOREST, JPMJFR220F) and the Japan Society for the Promotion of Science (KAKENHI 21H02125, 22H02270).

ACCEPTED MANUSCRIPT

Downloaded from https://academic.oup.com/jxb/advance-article/doi/10.1093/jxb/eraf285/8174788 by guest on 10 July 2025

Data availability statement

All data are presented in the article and supplementary figures.

References

Ablazov A, Jamil M, Haider I, Wang JY, Melino V, Maghrebi M, Vigani G, Liew KX, Lin PY, Chen GE, Kuijer HNJ, Berqdar L, Mazzarella T, Fiorilli V, Lanfranco L, Zheng X, Dai NC, Lai MH, Caroline Hsing YI, Tester M, Blilou I, Al-Babili S. 2024. *Zaxinone Synthase* overexpression modulates rice physiology and metabolism, enhancing nutrient uptake, growth and productivity. Plant, Cell & Environment **47**, 3647–3661.

Arite T, Umehara M, Ishikawa S, Hanada A, Maekawa M, Yamaguchi S, Kyozuka J. 2009. *d14*, a Strigolactone-Insensitive Mutant of Rice, Shows an Accelerated Outgrowth of Tillers. Plant and Cell Physiology **50**, 1416-1424.

Beveridge CA, Symons GM, Murfet IC, Ross JJ, Rameau C. 1997. The *rms1* Mutant of Pea Has Elevated Indole-3-Acetic Acid Levels and Reduced Root-Sap Zeatin Riboside Content but Increased Branching Controlled by Graft-Transmissible Signal(s). Plant Physiology **115**, 1251-1258.

Brewer PB, Koltai H, Beveridge CA. 2013. Diverse roles of strigolactones in plant development. Molecular Plant **6**, 18-28.

Brewer PB, Yoneyama K, Filardo F, Meyers E, Scaffidi A, Frickey T, Akiyama K, Seto Y, Dun EA, Cremer JE, Kerr SC, Waters MT, Flematti GR, Mason MG, Weiller G, Yamaguchi S, Nomura T, Smith SM, Yoneyama K, Beveridge CA. 2016. *LATERAL BRANCHING OXIDOREDUCTASE* acts in the final stages of strigolactone biosynthesis in Arabidopsis. Proceedings of the National Academy of Sciences, USA **113**, 6301-6306.

Chen GE, Wang JY, Votta C, Braguy J, Jamil M, Kirschner GK, Fiorilli V, Berqdar L, Balakrishna A, Blilou I, Lanfranco L, Al-Babili S. 2023. Disruption of the rice *4-*

ACCEPTED MANUSCRIPT

Downloaded from https://academic.oup.com/jxb/advance-article/doi/10.1093/jxb/eraf285/8174788 by guest on 10 July 2025

DEOXYOROBANCHOL HYDROXYLASE unravels specific functions of canonical strigolactones. Proceedings of the National Academy of Sciences, USA **120**, e2306263120.

Clough SJ, Bent AF. 1998. Floral dip: a simplified method for Agrobacterium-mediated transformation of Arabidopsis thaliana. The Plant Journal **16**, 735-743.

Dun EA, Brewer PB, Gillam EMJ, Beveridge CA. 2023. Strigolactones and Shoot Branching: What Is the Real Hormone and How Does It Work? Plant and Cell Physiology **64**, 967-983.

Francis B, Aravindakumar CT, Brewer PB, Simon S. 2023. Plant nutrient stress adaptation: A prospect for fertilizer limited agriculture. Environmental and Experimental Botany **213**, 105431.

Giovannetti M, Mosse B. 1980. An Evaluation of Techniques for Measuring Vesicular Arbuscular Mycorrhizal Infection in Roots. New Phytologist **84**, 489–500.

Gomez-Roldan V, Fermas S, Brewer PB, Puech-Pagès V, Dun EA, Pillot JP, Letisse F, Matusova R, Danoun S, Portais JC, Bouwmeester H, Bécard G, Beveridge CA, Rameau C, Rochange SF. 2008. Strigolactone inhibition of shoot branching. Nature **455**, 189-194.

Grace EJ, Cotsaftis O, Tester M, Smith FA, Smith SE. 2009. Arbuscular mycorrhizal inhibition of growth in barley cannot be attributed to extent of colonization, fungal phosphorus uptake or effects on expression of plant phosphate transporter genes. New Phytologist **181**, 938-949.

Guan JC, Li C, Flint-Garcia S, Suzuki M, Wu S, Saunders JW, Dong L, Bouwmeester HJ, McCarty DR, Koch KE. 2023. Maize domestication phenotypes reveal strigolactone networks coordinating grain size evolution with kernel-bearing cupule architecture. The Plant Cell **35**, 1013-1037.

Haider I, Yunmeng Z, White F, Li C, Incitti R, Alam I, Gojobori T, Ruyter-Spira C, Al-Babili S, Bouwmeester HJ. 2023. Transcriptome analysis of the phosphate starvation response sheds light on strigolactone biosynthesis in rice. The Plant Journal **114**, 355-370.

Harwood WA. 2014. A Protocol for High-Throughput *Agrobacterium*-Mediated Barley Transformation. Methods in Molecular Biology **1099**, 251-260.

ACCEPTED MANUSCRIPT

Downloaded from https://academic.oup.com/jxb/advance-article/doi/10.1093/jxb/eraf285/8174788 by guest on 10 July 2025

Hellens AM, Chabikwa TG, Fichtner F, Brewer PB, Beveridge CA. 2023. Identification of new potential downstream transcriptional targets of the strigolactone pathway including glucosinolate biosynthesis. Plant Direct **7**, e486.

Huang X, Kuang Z, Zhou R, Liu T, Tang L, Gao Z, Liu T, Fan X, Xuan W, Luo L, Xu G. 2025. Mutation of strigolactone biosynthetic gene *DWARF 17* impairs the responses of rice tillering to N supply. Plant J **122**, e70124.

Inoue M, Xie X, Yoneyama K. 2024. Barley is a potential trap crop for root parasitic broomrape weeds. Journal of Pesticide Science **49**, 255-261.

Ito S, Braguy J, Wang JY, Yoda A, Fiorilli V, Takahashi I, Jamil M, Felemban A, Miyazaki S, Mazzarella T, Chen GE, Shinozawa A, Balakrishna A, Berqdar L, Rajan C, Ali S, Haider I, Sasaki Y, Yajima S, Akiyama K, Lanfranco L, Zurbriggen MD, Nomura T, Asami T, Al-Babili S. 2022. Canonical strigolactones are not the major determinant of tillering but important rhizospheric signals in rice. Science Advances **8**, eadd1278.

Kaur S, Campbell BJ, Suseela V. 2022. Root metabolome of plant-arbuscular mycorrhizal symbiosis mirrors the mutualistic or parasitic mycorrhizal phenotype. New Phytologist **234**, 672-687.

Kelly JH, Tucker MR, Brewer PB. 2023. The Strigolactone Pathway Is a Target for Modifying Crop Shoot Architecture and Yield. Biology (Basel) **12**, 95.

Kuijer HNJ, Wang JY, Bougouffa S, Abrouk M, Jamil M, Incitti R, Alam I, Balakrishna A, Alvarez D, Votta C, Chen GE, Martínez C, Zuccolo A, Berqdar L, Sioud S, Fiorilli V, de Lera AR, Lanfranco L, Gojobori T, Wing RA, Krattinger SG, Gao X, Al-Babili S. 2024. Chromosome-scale pearl millet genomes reveal *CLAMT1b* as key determinant of strigolactone pattern and Striga susceptibility. Nat Commun **15**, 6906.

Lailheugue V, Merlin I, Boutet S, Perreau F, Pouvreau JB, Delgrange S, Ducrot PH, Cottyn-Boitte B, Mouille G, Lauvergeat V. 2023. Vitislactone, a non-canonical strigolactone

ACCEPTED MANUSCRIPT

Downloaded from https://academic.oup.com/jxb/advance-article/doi/10.1093/jxb/eraf285/8174788 by guest on 10 July 2025

exudated by grapevine rootstocks in response to nitrogen starvation. Phytochemistry **215**, 113837.

Li C, Dong L, Durairaj J, Guan JC, Yoshimura M, Quinodoz P, Horber R, Gaus K, Li J, Setotaw YB, Qi J, De Groote H, Wang Y, Thiombiano B, Floková K, Walmsley A, Charnikhova TV, Chojnacka A, Correia de Lemos S, Ding Y, Skibbe D, Hermann K, Screpanti C, De Mesmaeker A, Schmelz EA, Menkir A, Medema M, Van Dijk ADJ, Wu J, Koch KE, Bouwmeester HJ. 2023. Maize resistance to witchweed through changes in strigolactone biosynthesis. Science **379**, 94-99.

Li C, Haider I, Wang JY, Quinodoz P, Suarez Duran HG, Méndez LR, Horber R, Fiorilli V, Votta C, Lanfranco L, Correia de Lemos SM, Jouffroy L, Moegle B, Miesch L, De Mesmaeker A, Medema MH, Al-Babili S, Dong L, Bouwmeester HJ. 2024. OsCYP706C2 diverts rice strigolactone biosynthesis to a noncanonical pathway branch. Science Advances **10**, eadq3942.

Ma X, Zhang Q, Zhu Q, Liu W, Chen Y, Qiu R, Wang B, Yang Z, Li H, Lin Y, Xie Y, Shen R, Chen S, Wang Z, Chen Y, Guo J, Chen L, Zhao X, Dong Z, Liu YG. 2015. A Robust CRISPR/Cas9 System for Convenient, High-Efficiency Multiplex Genome Editing in Monocot and Dicot Plants. Molecular Plant **8**, 1274-1284.

Marzec M, Daszkowska-Golec A, Collin A, Melzer M, Eggert K, Szarejko I. 2020a. Barley strigolactone signalling mutant *hvd14.d* reveals the role of strigolactones in abscisic acid-dependent response to drought. Plant, Cell & Environment **43**, 2239-2253.

Marzec M, Gruszka D, Tylec P, Szarejko I. 2016. Identification and functional analysis of the *HvD14* gene involved in strigolactone signaling in *Hordeum vulgare*. Physiologia Plantarum **158**, 341-355.

Marzec M, Situmorang A, Brewer PB, Braszewska A. 2020b. Diverse Roles of MAX1 Homologues in Rice. Genes (Basel) **11**, 1348.

ACCEPTED MANUSCRIPT

Downloaded from https://academic.oup.com/jxb/advance-article/doi/10.1093/jxb/eraf285/8174788 by guest on 10 July 2025

Mascher M, Wicker T, Jenkins J, Plott C, Lux T, Koh CS, Ens J, Gundlach H, Boston LB, Tulpová Z, Holden S, Hernández-Pinzón I, Scholz U, Mayer KFX, Spannagl M, Pozniak CJ, Sharpe AG, Šimková H, Moscou MJ, Grimwood J, Schmutz J, Stein N. 2021. Long-read sequence assembly: a technical evaluation in barley. The Plant Cell **33**, 1888-1906.

Mashiguchi K, Seto Y, Onozuka Y, Suzuki S, Takemoto K, Wang Y, Dong L, Asami K, Noda R, Kisugi T, Kitaoka N, Akiyama K, Bouwmeester H, Yamaguchi S. 2022. A carlactonoic acid methyltransferase that contributes to the inhibition of shoot branching in *Arabidopsis*. Proceedings of the National Academy of Sciences, USA **119**, e2111565119.

Mizutori Y, Nishiyama K, Seto Y. 2025. Inhibition of shoot branching in Arabidopsis by the artificially produced canonical-strigolactone. Bioscience, Biotechnology, and Biochemistry, zbae202.

Mori N, Nomura T, Akiyama K. 2020. Identification of two oxygenase genes involved in the respective biosynthetic pathways of canonical and non-canonical strigolactones in *Lotus japonicus*. Planta **251**, 40.

Moriyama D, Wakabayashi T, Shiotani N, Yamamoto S, Furusato Y, Yabe K, Mizutani M, Takikawa H, Sugimoto Y. 2022. Identification of 6-*epi*-heliolactone as a biosynthetic precursor of avenaol in *Avena strigosa*. Bioscience, Biotechnology, and Biochemistry **86**, 998-1003.

Nomura T, Seto Y, Kyozuka J. 2024. Unveiling the complexity of strigolactones: exploring structural diversity, biosynthesis pathways, and signaling mechanisms. Journal of Experimental Botany **75**, 1134-1147.

Pribil M, Pesaresi P, Hertle A, Barbato R, Leister D. 2010. Role of plastid protein phosphatase TAP38 in LHCII dephosphorylation and thylakoid electron flow. PLoS Biol **8**, e1000288.

Salam BB, Barbier F, Danieli R, Teper-Bamnolker P, Ziv C, Spichal L, Aruchamy K, Shnaider Y, Leibman D, Shaya F, Carmeli-Weissberg M, Gal-On A, Jiang J, Ori N,

ACCEPTED MANUSCRIPT

Downloaded from https://academic.oup.com/jxb/advance-article/doi/10.1093/jxb/eraf285/8174788 by guest on 10 July 2025

Beveridge C, Eshel D. 2021. Sucrose promotes stem branching through cytokinin. Plant Physiology **185**, 1708-1721.

Sigalas PP, Bennett T, Buchner P, Thomas SG, Jamois F, Arkoun M, Yvin JC, Bennett MJ, Hawkesford MJ. 2024. At the crossroads: strigolactones mediate changes in cytokinin synthesis and signalling in response to nitrogen limitation. Plant J **120**, 139-158.

Sparkes IA, Runions J, Kearns A, Hawes C. 2006. Rapid, transient expression of fluorescent fusion proteins in tobacco plants and generation of stably transformed plants. Nature Protocols **1**, 2019-2025.

Sun H, Guo X, Zhu X, Gu P, Zhang W, Tao W, Wang D, Wu Y, Zhao Q, Xu G, Fu X, Zhang Y. 2023. Strigolactone and gibberellin signaling coordinately regulate metabolic adaptations to changes in nitrogen availability in rice. Molecular Plant **16**, 588-598.

Szurman-Zubrzycka M, Chmielewska B, Gajewska P, Szarejko I. 2017. Mutation Detection by Analysis of DNA Heteroduplexes in TILLING Populations of Diploid Species. In: Jankowicz-Cieslak J, Tai TH, Kumlehn J, Till BJ, eds. *Biotechnologies for Plant Mutation Breeding*. Cham.: Springer, 281–303.

Szurman-Zubrzycka ME, Zbieszczyk J, Marzec M, Jelonek J, Chmielewska B, Kurowska MM, Krok M, Daszkowska-Golec A, Guzy-Wrobelska J, Gruszka D, Gajecka M, Gajewska P, Stolarek M, Tylec P, Sega P, Lip S, Kudelko M, Lorek M, Gorniak-Walas M, Malolepszy A, Podsiadlo N, Szyrajew KP, Keisa A, Mbambo Z, Todorowska E, Gaj M, Nita Z, Orlowska-Job W, Maluszynski M, Szarejko I. 2018. *Hor*TILLUS-A Rich and Renewable Source of Induced Mutations for Forward/Reverse Genetics and Pre-breeding Programs in Barley (*Hordeum vulgare* L.). Frontiers in Plant Science **9**, 216.

Tadano T, Tanaka A. 1980. The effect of low phosphate concentrations in culture medium on early growth of several crop plant (in Japanese, translated by the authors). Japanese Journal of Soil Science and Plant Nutrition **51**, 399–404.

ACCEPTED MANUSCRIPT

Downloaded from https://academic.oup.com/jxb/advance-article/doi/10.1093/jxb/eraf285/8174788 by guest on 10 July 2025

Umehara M, Hanada A, Yoshida S, Akiyama K, Arite T, Takeda-Kamiya N, Magome H, Kamiya Y, Shirasu K, Yoneyama K, Kyozuka J, Yamaguchi S. 2008. Inhibition of shoot branching by new terpenoid plant hormones. Nature **455**, 195-200.

Verwoerd TC, Dekker BM, Hoekema A. 1989. A small-scale procedure for the rapid isolation of plant RNAs. Nucleic Acids Research **17**, 2362.

Vierheilig H, Coughlan AP, Wyss U, Piche Y. 1998. Ink and vinegar, a simple staining technique for arbuscular-mycorrhizal fungi. Applied and Environmental Microbiology **64**, 5004-5007.

Wakabayashi T, Hamana M, Mori A, Akiyama R, Ueno K, Osakabe K, Osakabe Y, Suzuki H, Takikawa H, Mizutani M, Sugimoto Y. 2019. Direct conversion of carlactonoic acid to orobanchol by cytochrome P450 CYP722C in strigolactone biosynthesis. Science Advances **5**, eaax9067.

Wakabayashi T, Yasuhara R, Miura K, Takikawa H, Mizutani M, Sugimoto Y. 2021. Specific methylation of (11R)-carlactonoic acid by an Arabidopsis SABATH methyltransferase. Planta **254**, 88.

Wang H, Chen W, Eggert K, Charnikhova T, Bouwmeester H, Schweizer P, Hajirezaei MR, Seiler C, Sreenivasulu N, von Wiren N, Kuhlmann M. 2018. Abscisic acid influences tillering by modulation of strigolactones in barley. Journal of Experimental Botany **69**, 3883-3898.

Wang JY, Chen GE, Braguy J, Al-Babili S. 2024. Distinguishing the functions of canonical strigolactones as rhizospheric signals. Trends in Plant Science **29**, 925-936.

Waters MT, Nelson DC, Scaffidi A, Flematti GR, Sun YK, Dixon KW, Smith SM. 2012. Specialisation within the DWARF14 protein family confers distinct responses to karrikins and strigolactones in *Arabidopsis*. Development **139**, 1285-1295.

Wu K, Wang S, Song W, Zhang J, Wang Y, Liu Q, Yu J, Ye Y, Li S, Chen J, Zhao Y, Wang J, Wu X, Wang M, Zhang Y, Liu B, Wu Y, Harberd NP, Fu X. 2020. Enhanced sustainable

ACCEPTED MANUSCRIPT

Downloaded from https://academic.oup.com/jxb/advance-article/doi/10.1093/jxb/eraf285/8174788 by guest on 10 July 2025

green revolution yield via nitrogen-responsive chromatin modulation in rice. Science **367**, eaaz2046.

Xie X, Yoneyama K, Kisugi T, Nomura T, Akiyama K, Asami T, Yoneyama K. 2016. Structure- and stereospecific transport of strigolactones from roots to shoots. J Pestic Sci **41**, 55-58.

Yamada Y, Otake M, Furukawa T, Shindo M, Shimomura K, Yamaguchi S, Umehara M. 2019. Effects of Strigolactones on Grain Yield and Seed Development in Rice. Journal of Plant Growth Regulation **38**, 753–764.

Yamaguchi A, Wu MF, Yang L, Wu G, Poethig RS, Wagner D. 2009. The microRNA-regulated SBP-Box transcription factor SPL3 is a direct upstream activator of *LEAFY*, *FRUITFULL*, and *APETALA1*. Dev Cell **17**, 268-278.

Yoneyama K, Akiyama K, Brewer PB, Mori N, Kawano-Kawada M, Haruta S, Nishiwaki H, Yamauchi S, Xie X, Umehara M, Beveridge CA, Yoneyama K, Nomura T. 2020a. Hydroxyl carlactone derivatives are predominant strigolactones in *Arabidopsis*. Plant Direct **4**, e00219.

Yoneyama K, Brewer PB. 2021. Strigolactones, how are they synthesized to regulate plant growth and development? Current Opinion in Plant Biology **63**, 102072.

Yoneyama K, Xie X, Nomura T, Yoneyama K. 2020b. Do Phosphate and Cytokinin Interact to Regulate Strigolactone Biosynthesis or Act Independently? Frontiers in Plant Science **11**, 438.

Yoneyama K, Xie X, Nomura T, Yoneyama K, Bennett T. 2022. Supra-organismal regulation of strigolactone exudation and plant development in response to rhizospheric cues in rice. Current Biology **32**, 3601-3608 e3603.

Zhang J, Mazur E, Balla J, Gallei M, Kalousek P, Medveďová Z, Li Y, Wang Y, Prat T, Vasileva M, Reinöhl V, Procházka S, Halouzka R, Tarkowski P, Luschnig C, Brewer PB, Friml J. 2020. Strigolactones inhibit auxin feedback on PIN-dependent auxin transport canalization. Nature Communications **11**, 3508.

ACCEPTED MANUSCRIPT

Downloaded from https://academic.oup.com/jxb/advance-article/doi/10.1093/jxb/eraf285/8174788 by guest on 10 July 2025

Zhou A, Kane A, Wu S, Wang K, Santiago M, Ishiguro Y, Yoneyama K, Palayam M, Shabek N, Xie X, Nelson DC, Li Y. 2025. Evolution of interorganismal strigolactone biosynthesis in seed plants. Science **387**, eadp0779.

Tables

Table 1. *HvLBO* alleles isolated from screening of *Hor*TILLUS mutagenized population.

Allele	Nucleotide change (from ATG)	Effect	Mutation type
lbo.d	G815A	D241N	missense
lbo.e	G834A	S247N	missense
lbo.f	G845A	D251N	missense
lbo.ia	C915T	A274V	missense

Figure legends

Fig. 1. Analysis of the *hvlbo.f* mutant. (A) *HvLBO* encodes a 2-oxoglutarate and Fe(II)-dependent dioxygenase (2-OGD) across two exons, including a conserved double-stranded β-helix conserved catalytic domain (DSBH). A start codon was predicted (pale arrow). However, a second site is likely the real start codon (arrow), because this matches the protein sequence of BAJ96311 derived from a full length cDNA library, which we confirmed by PCR of a cDNA sample. The locations of three independent mutant alleles are shown (arrowheads) (an in-frame mutation, *hvlbo-1*, was not included in this study). (B) A *35S:HvLBO* construct was transformed into the *atlbo-1* mutant allele of Arabidopsis. The rosette branch number was reduced to WT (Ws-4) levels in four independent transgenic T3 lines. Data are mean ± SEM, n = 23-26. (C) Primers specific for *HvLBO* were used to detect relative expression of the transgene in independent plants from each T3 line. Data are mean ± SEM, n = 3. (D) Mutant *hvlbo.f* plants isolated from the *Hor*TILLUS TILLING population showed increased tiller number

ACCEPTED MANUSCRIPT

Downloaded from https://academic.oup.com/jxb/advance-article/doi/10.1093/jxb/eraf285/8174788 by guest on 10 July 2025

compared to the WT Sebastian cultivar (Seb) during the later phase of growth, but not earlier. Data are mean ± SEM, *n* = 19-27. (E) Plant height was reduced in *hvlbo.f*. Data are mean ± SEM, *n* = 19-27. (F) A 35S construct expressing the barley mutant *hvlbo.f* CDS was also transformed into the *atlbo-1* mutant of Arabidopsis. The rosette branch number was only partially reduced to WT (Ws-4) levels in two out of four independent transgenic T3 lines. Data are mean ± SEM, *n* = 23-27. (G) Primers specific for *HvLBO*/*hvlbo.f* were used to detect relative expression of the transgene in independent plants from each T3 line. Data are mean ± SEM, *n* = 3. Different letters indicate statistically significant differences by one-way ANOVA Tukey's test, $P < 0.05$. Asterisks show significant differences by student's *t*-test, **** $P \leq 0.0001$.

Fig. 2. Analysis of *hvlbo* gene edited mutants. (A) Mutant *hvlbo-2* and *hvlbo-3* plants grown in hydroponic cups. Red arrowheads indicate tillers. (B) Mutant *hvlbo-2 and hvlbo-3* plants showed increased tillering at 18 days old compared to the WT variety (Golden promise (GP)), but not as much as *hvd14.d* (compared to WT Sebastian (Seb)). (C) In pots with soil and normal nutrients, *hvlbo-2* tiller number was not different in at 33 days post emergence, but became greater in older plants. Root tissue was collected from the plants in hydroponic cups at 28 days old, after 10 days of P starvation. Extracts from the root tissues were analyzed for SLs by LC-MS/MS. (D) 6-*Epi*-heliolactone was detected in the WTs and mutants, at similar relative levels. (E) Barleylactone 2 was detected in the WTs and mutants, at similar levels. Other SLs were not detected. (F) Root biomass was not significantly different. Data are mean ± SEM, *n* = 4-8. Asterisks show significant differences by student's *t*-test, * $P \leq 0.05$, ** $P \leq 0.01$.

ACCEPTED MANUSCRIPT

Downloaded from https://academic.oup.com/jxb/advance-article/doi/10.1093/jxb/eraf285/8174788 by guest on 10 July 2025

Fig. 3: *hvlbo* mutant phenotype on low (250 mg/kg soil), intermediate (500 mg/kg) and normal (750 mg/kg) nitrate (N) added at sowing, compared to WT (Golden Promise). (A) *hvlbo-2* mutant tiller number, (B) grains per plant, (C) yield per plant, (D) average grain (kernel) mass per plant, (E) harvest index (yield as a proportion of total shoot biomass), (F) Percentage of seed set (a grain present) at each seed position, (G) total shoot biomass including grains, and (H) plant height. Data are mean ± SEM, n = 10. Different letters indicate statistically significant differences by two-way ANOVA Tukey's test, $P < 0.05$.

Fig. 4. The effects of SL treatment and AM fungal inoculation (*Rhizophagus irregularis*) on barley *hvlbo* mutants. (A) Doses of 2µM *rac*-GR24 repressed tiller number in *hvlbo-2* but not WT Golden Promise (GP). Data are mean ± SEM, n = 10. (B) The percentage presence of each of AM hyphae, vesicles and arbuscules were not obviously different between WT Golden Promise (GP), *hvlbo-2* and *hvlbo-3* at 48 dpi. Data are mean ± SEM, n = 6. (C) Shoot fresh weight at 34 dpi trended upwards in the mutants compared to WT (GP), and downwards with AM fungal inoculation. (D) Root fresh weight trended downwards in both the mutants and with AM fungal inoculation. Data are mean ± SEM, n = 5-6. Different letters indicate statistically significant differences by two-way ANOVA Tukey's test, $P < 0.05$.

Fig. 5. *lbo* mutant plants grown in hydroponics with phosphorus (-P) or nitrogen (-N) starvation conditions. SL exudates analyzed by LC-MS/MS. WT (Golden promise; GP)

ACCEPTED MANUSCRIPT

Downloaded from https://academic.oup.com/jxb/advance-article/doi/10.1093/jxb/eraf285/8174788 by guest on 10 July 2025

and mutant show similar large increases in (A) 6-*epi*-heliolactone and (B) barleylactone 2. Data are mean ± SEM, *n* = 2-5. SL exudate collected samples were also applied to parasitic weed seeds, (C) Branched broomrape (*Phelipanche ramosa*) and (D) Egyptian broomrape (*Phelipanche aegyptiaca*), and assessed for percentage germination. Data are mean ± SEM, *n* = 9. Not significant (ns) is as per two-way ANOVA Tukey's test, $P > 0.05$.

ACCEPTED MANUSCRIPT

Downloaded from https://academic.oup.com/jxb/advance-article/doi/10.1093/jxb/eraf285/8174788 by guest on 10 July 2025

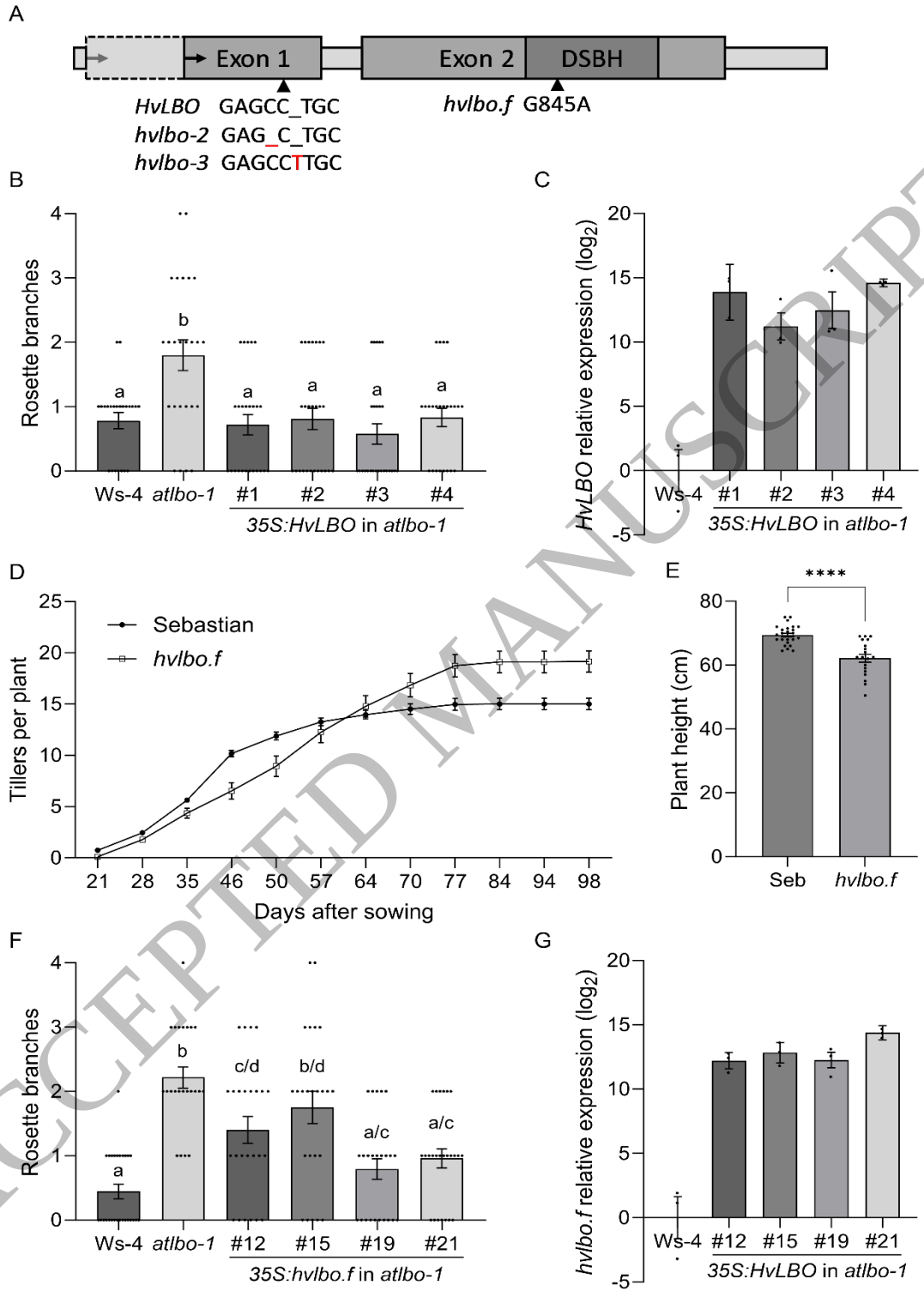

Figure 1
159x219 mm (x DPI)

ACCEPTED MANUSCRIPT

Downloaded from https://academic.oup.com/jxb/advance-article/doi/10.1093/jxb/eraf285/8174788 by guest on 10 July 2025

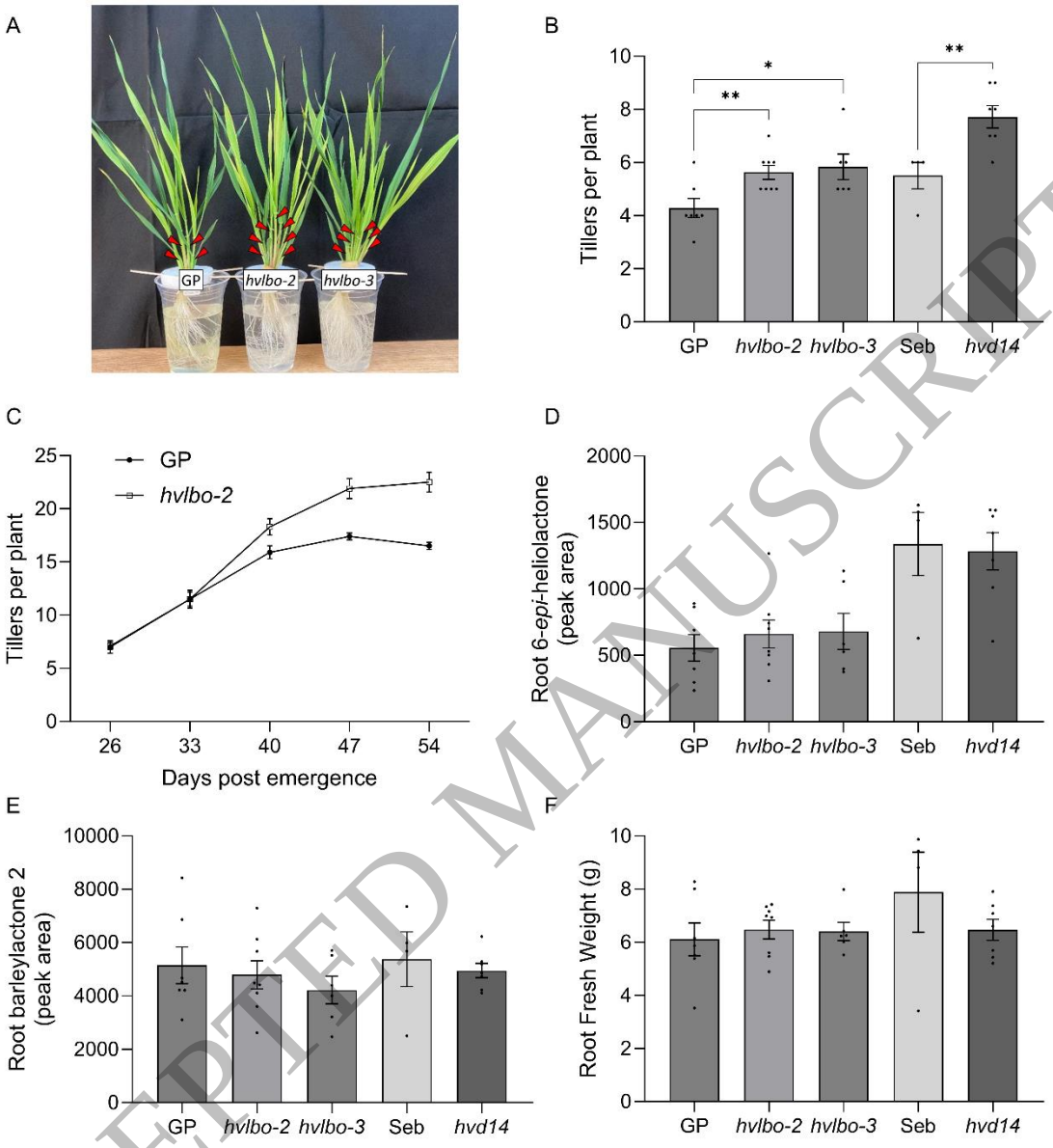

Figure 2
159x163 mm (x DPI)

ACCEPTED MANUSCRIPT

Downloaded from https://academic.oup.com/jxb/advance-article/doi/10.1093/jxb/eraf285/8174788 by guest on 10 July 2025

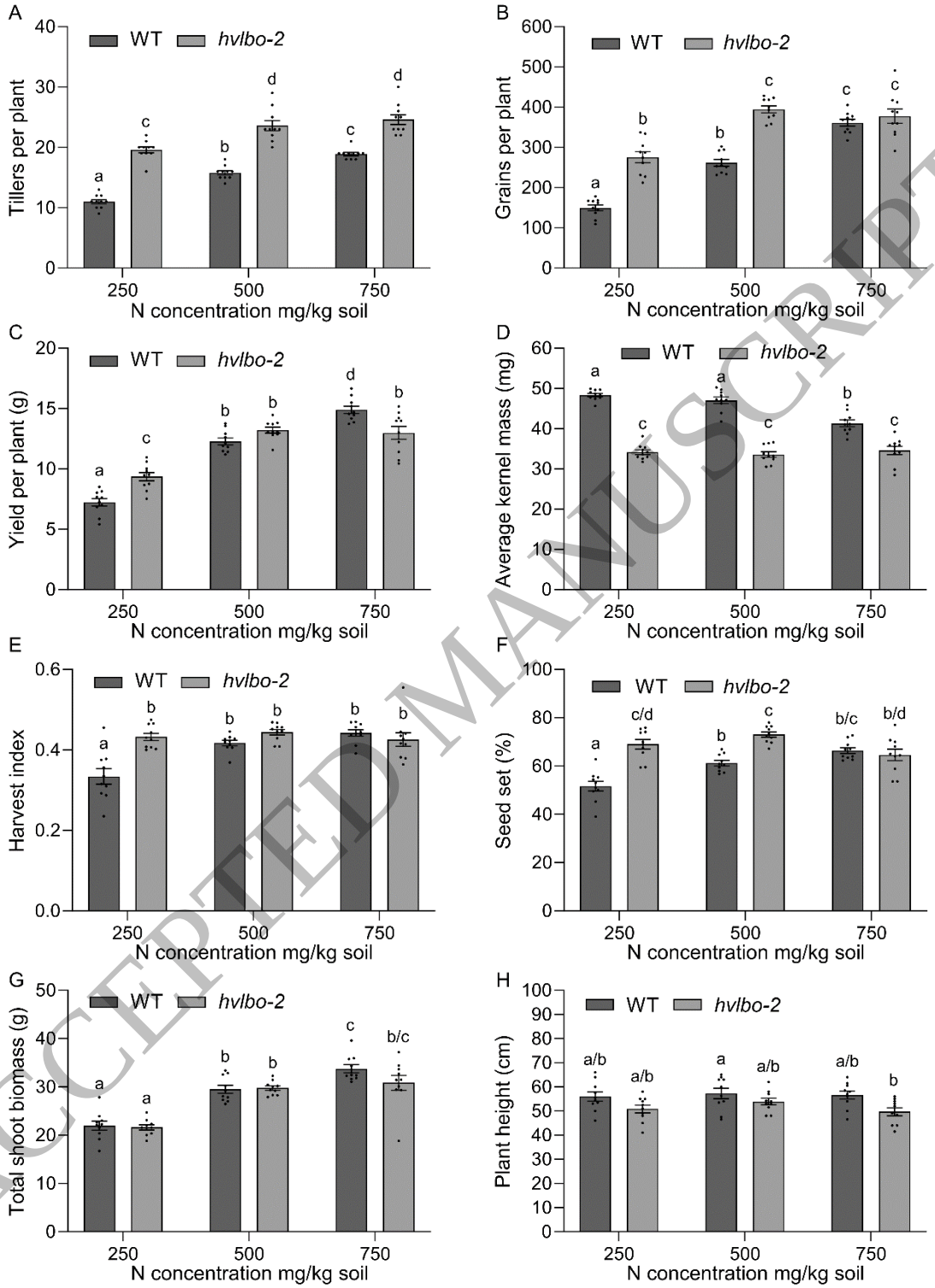

Figure 3
159x208 mm (x DPI)

ACCEPTED MANUSCRIPT

Downloaded from https://academic.oup.com/jxb/advance-article/doi/10.1093/jxb/eraf285/8174788 by guest on 10 July 2025

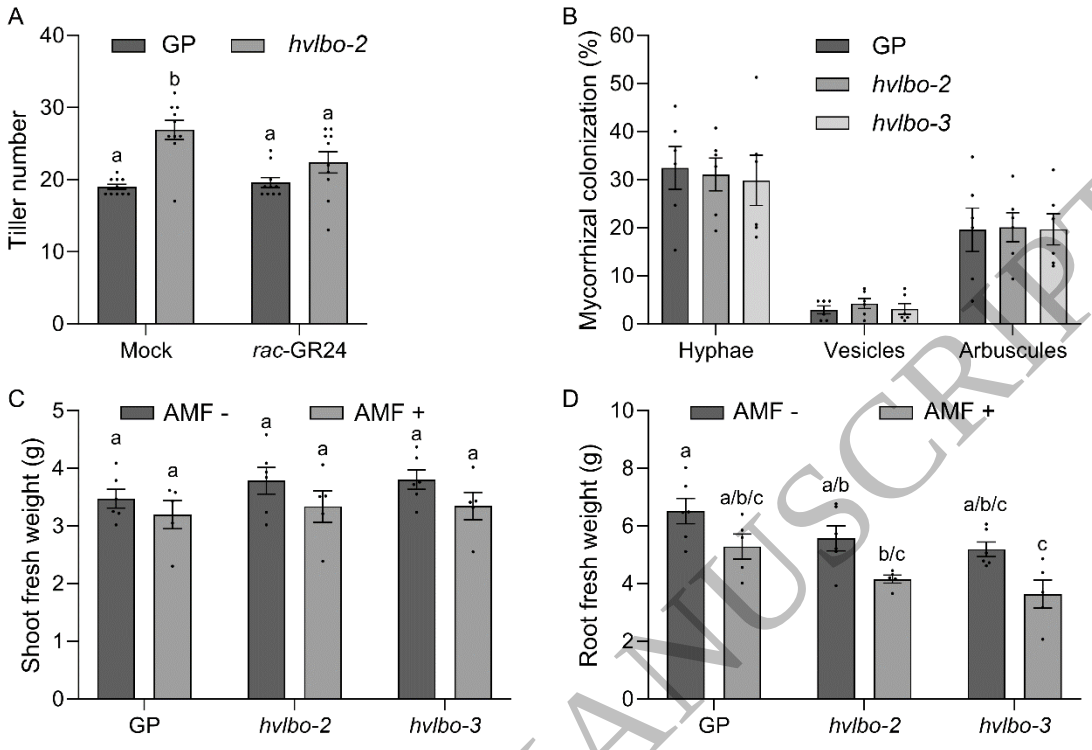

Figure 4
159x105 mm (x DPI)

ACCEPTED MANUSCRIPT

Downloaded from https://academic.oup.com/jxb/advance-article/doi/10.1093/jxb/eraf285/8174788 by guest on 10 July 2025

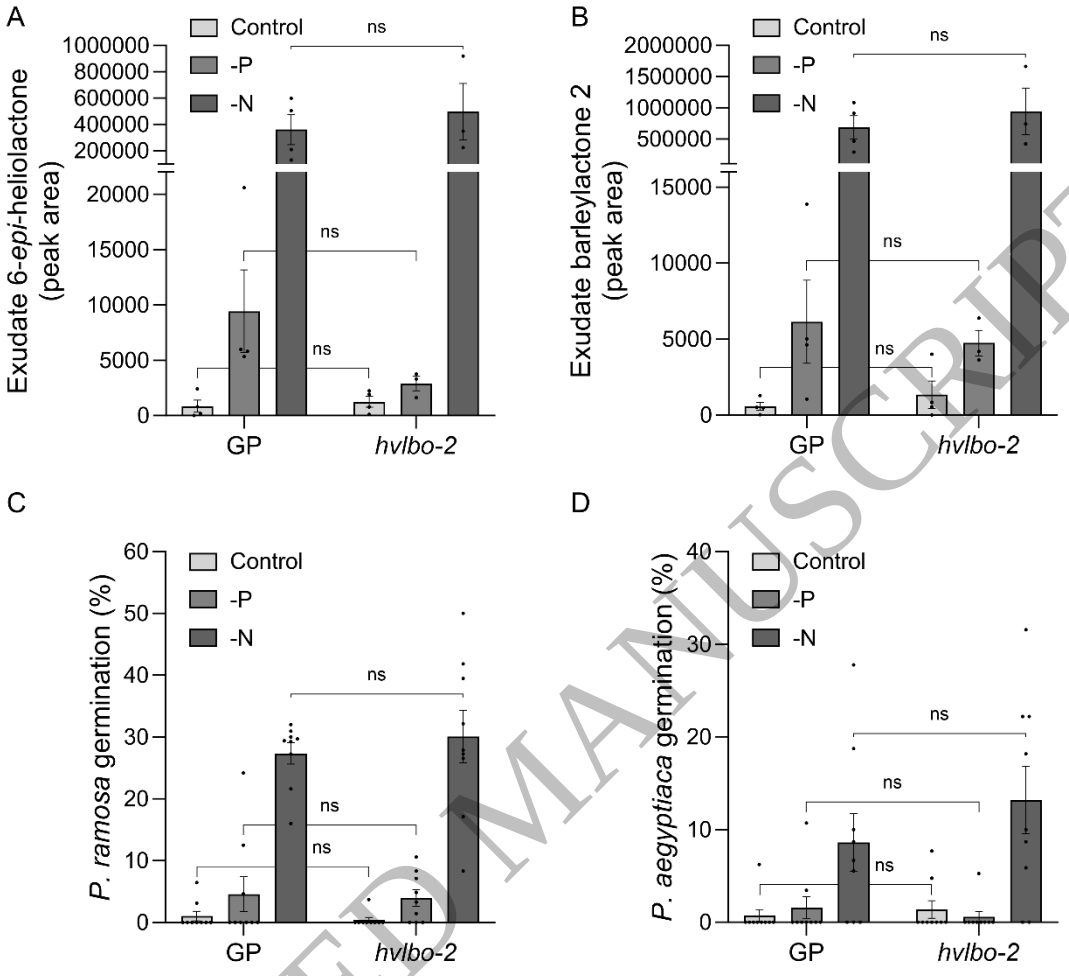

Figure 5
159x138 mm (x DPI)

ACCEPTED MANUSCRIPT

Downloaded from https://academic.oup.com/jxb/advance-article/doi/10.1093/jxb/eraf285/8174788 by guest on 10 July 2025